



Various Material Development Strategies for Suitable Catalysts of Photo Catalytic Water Splitting to Green Fuel H₂:A Critical Review

MD. SAHAB UDDIN, MD. ABDUS SALAM*, MD. SHEHAN HABIB,
KAWSAR AHMED, TAREQ HOSSAIN and NASRIN PAPRI

Hydrogen Energy Laboratory, BCSIR Laboratories, Chittagong-4220, Bangladesh.

Abstract

Fossil fuels are the most substantial & extensively used sources of energy for today's world. Simultaneously, the unconscious exposure of toxic pollutants and green-house gases allied with fossil energy is not viable with contexture. Solar energy were treated as an auspicious source of energy from ancient age because of its richness & cleanness. But problem arises in its capture, storage, transformation, and distribution. That's why scholars are trying to convert this renewable light energy to a user friendly and viable form of energy. By analyzing recent studies on H₂ fuel it is considered as most lucrative choice for clean and sustainable fuel with high calorific value & zero pollution. This review offers an overview of most recent advancement in development of photo-catalyst for solar water splitting which is treated as a promising Green-Harvesting technique among all H₂ generation techniques. Here we discussed about various catalyst development techniques especially about doping techniques, reactor design and light scattering/trapping systems. We found that among all doping is a promising technique and a lots of study have been done on this technique than others like as Heterojunction, Dye sensitization, modification of surface or nanostructure formation. Hence we concluded with the decision that, more research are needed on heterojunction and nanostructure formation along with elemental doping.



Article History

Received: 19 March 2020

Accepted: 25 April 2021

Keywords

Catalyst;
Doping;
Dye Sensitization;
Hydrogen;
Heterojunction;
Photo-Catalyst;
Solar Fuels;
Water Splitting.

Introduction

The high energy crisis, fossil fuels depletion & environment pollution becoming the major global challenges in recent and upcoming years.¹ Due to

global warming & pollution issues, today's world is searching for a sustainable, clean, and environment friendly alternatives. With a vast study on fuel and its negative impacts, scientists came to know that,

CONTACT Md. Abdus Salam ✉ salam.helc@ctghelc.com.bd 📍 Hydrogen Energy Laboratory, BCSIR Laboratories, Chittagong-4220, Bangladesh.



© 2021 The Author(s). Published by Enviro Research Publishers.

This is an Open Access article licensed under a Creative Commons license: Attribution 4.0 International (CC-BY).

Doi: <http://dx.doi.org/10.13005/msri/180202>

hydrogen fuel may be a solution for this crisis. H₂ is a fantastic energy conveyer with a high CV and clean property. As a bountiful element, H₂ appear in many substances in the earth likely seawater, Biogas, freshwater and fossil fuels, etc. For the production of H₂ with zero or low impact on the environment, almost all Carbon-dioxide with other unwanted particulates should be separated when H₂ is produced from fossils.² Till now, hydrogen is mainly synthesized via steam reforming method where CO₂ is formed simultaneously. And this CO₂ is the key concern for today's environmentalists, as it is the major greenhouse agent. Photo-catalytic water splitting may be a solution to these problems. Some other important sources of the hydrogen production process are Electrolysis, Thermochemical processes, Dark fermentation process, Thermolysis, Photo-fermentation or Bio-photolysis, Hybrid thermochemical cycles, and Photo-catalytic water splitting, etc. For ultra-pure H₂ production, electrolysis is a more reliable, technically sound, and widely acceptable system. Electrolysis is a technique where direct current (DC) is used to drive the anion-spontaneous electrochemical reaction.³ To run this technique, immaculate power hubs may be engaged like as solar-powered energy, geothermal based energy, biogas energy, wind-powered energy, ocean and others. The energy produced from nuclear energy sources may also be used for driving this process. Hydrogen produces in this technique is purer than any other technique, O₂ production was also high in this technique. But the major disadvantage of this technique is that a huge amount of electricity is needed to run the electrolysis technique and the initial set-up cost is expensive in amount. The major reaction involve with the electrolytic technique of water is generally written as:



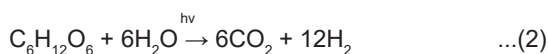
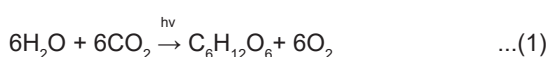
On the other hand, thermochemical processes are another convincing process for hydrogen production. The thermochemical system is the process which mainly driven by heat as its primary energy. This type of process for the production of hydrogen is considered as the viable process for the probable alternative of the previous one. Most alluring support from thermochemical production cycles is no requirement of catalysts or agents to drive the process reactions.⁴ All chemicals, without water (main raw material), used here can

be reused easily. Other mesmerizing support of these types of degradation process are: (a) H₂ and O₂ can be separate from mixture gas without membrane; (b) optimum energy requirement range of 327–927°C; & (c) less electrical power consumption. This requirement of power can be provided by concentric solar energy, the geothermal energy, biogas, nuclear electricity, and other sources.⁵ But the challenges of this technique is that the bulk amount of heat supply source is not available in everywhere and artificially generation of heat is also costly. Here alleviate temperature degradation of catalyst is a major challenge, which retard the hydrogenproduction rate.

On the other hand, thermolysis is another significant way of electrolysis where H₂O is split to H₂ and O₂ at elevated temperatures ranging between 973K to 1273K. Basically this process is more effective than generally used room-temperature splitting process where efficiency increases with the increment of heat. The electrical energy needed here is much less than the conventional methods. Zero GHG emission is possible here by using the clean source of energy like solar, geological, wind or nuclear.⁶ Heat recovered from another process (such as industrial boiler or heat exchanger) can also be effectively used to run this process.⁷ In high temperatures operating system, the process units must have met some definite requirements for effective H₂ production. Most recent objections of these types of the process can be enlisted as: (a) stable electrolytic reagent synthesis with low electronic and strong ionic conductivity; (b) porous, low cost and chemically static electrode development for high electronic conductivity and finally (c) mechanically stable engineering materials at high temperatures. Again, Hybrid thermo-chemical cycles which conduct at low temperature is more viable while comparing with the thermally driven water-splitting system. Electrical and thermal energies fulfill the outer energy demand of particular reactions as hybrid systems conducted at lower temperatures. A major advantage of these types of systems is that H₂ generation from low-grade energy sources. But the major findings of this technique are that bulk amount heat source is not available everywhere and artificial generation of heat is also costly.

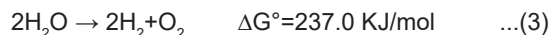
Bio-photolysis as well as photo-fermentation techniques are familiar as photon-based biochemical

H₂ generation from water. The main privilege of this technique is the capability to generate H₂ from H₂O in aqueous media at conditioned temperature & pressure.⁸ Here in the Bio photolysis processes light-sensitive micro-organisms are used as biological converters in a special bioreactor. Here Microalgae are most preferable among all microbes because they are culturable in suitable media.⁹ Cultured microalgae isolates have the capacity to produce H₂ in a closed system and they show high H₂ yields. The primary hydrogen generation reactions using photo-activated enzymes are the following:



However, this process is demonstrated at laboratory scale only and piloting is not yet possible to support the industries at the commercial level. Again Dark fermentation is a fermentation process which defined as the transformation of biochemical energy of organic to different forms of energy in dark conditions (during the reduced supply of light). In this process biochemical energy available in organic matter used to obtain H₂ in absence of light.¹⁰ Bioreactors used in these types of fermentation are cheaper and simpler in comparison with photo-fermentation because this method does not need solar input processing. There are several other benefits of H₂ production by dark fermentation like, (1) H₂ production from organic waste and (2) stabilized & control in bio-waste for reducing potential danger of pollution.¹¹ The dark fermentation process can be implemented in water treatment units for H₂ production from organic wastewater. H₂ production costs can be reduced by using inexpensive and readily available organic wastes (including wastewater). But the major disadvantage of this method is that the hydrogen production rate is very low and huge amount of reagents are required for continuous fermentation process which are non-recyclable.

From all available H₂ production the process discussed here photo-catalytic water splitting using sunlight has been widely believed as a promising process for green and environment-friendly hydrogen generation, where a chemical reaction occur while following with the alteration of Gibbs free energy (Eq. - 3).¹²



This type of Water Splitting has harmony with photosynthesis because both of them are uphill type. From this site, the water-splitting system can be evaluated as artificial photosynthesis. The utilization of green, inexhaustible and sustainable solar energy is an urgent need to avoid the greenhouse effects. A huge amount of research articles are circulating every year on solar energy transformation systems like photo-catalytic conversion of organic pollutants, hydrogen (H₂) gas production through photo-catalytic water splitting, photovoltaic cells, and dye-sensitized solar cells.¹³ Photo-electrochemical water splitting process by Fujishima & Honda in the year of 1972 is most variant of this technique.¹⁴ Following this way, till now H₂ production by Photocatalytic water splitting is considered as a promising technology for green energy revolution.¹⁵⁻¹⁷ (TiO₂) titanium oxide,¹⁸⁻²⁰ (g-C3N4) Graphitic-Carbon Nitride²¹⁻²³ and (CdS) Cadmium Sulfide²⁴⁻²⁶ are three widely studied catalysts for water splitting in the last few decades. Among them, titanium oxide (TiO₂) is found to be more superior, and a benchmark photo-catalyst still now.²⁷

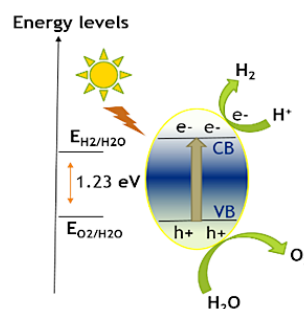
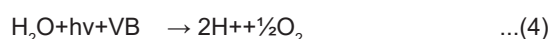
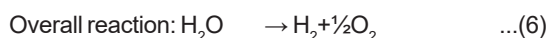


Fig.1: Photo-catalytic H₂ production using suitable semiconductor²⁸

Due to its photostability, efficiency, band edge, non-toxicity and sustainability it became a burning topic in this sector.²⁹⁻³⁴ The mechanism of Photocatalytic activity of TiO₂ based catalyst for water splitting are illustrated in Fig. 1.0.³⁵ The overall water splitting reaction on a photo-catalyst comprised of the following half reactions:





Herein, an overview of current development in photocatalyst, a comparison of different water splitting processes, various catalyst development techniques especially doping on composite matrix, its effect on hydrogen production and various types of doping technique are critically explained. Different techniques for catalyst development including

doping, Heterojunction, Dye sensitization, etc. are explained here. A complete study on doping is discussed here from all of its aspects. The numerous factors that affect the photo-catalytic water splitting such as band gaps, morphology, temperature, light intensity, pH, oxygen vacancies, and activity of sacrificial reagents are then scrutinously discussed here. Additionally, the reactor phenomenon and their commendation to further modification for H₂ production are also explained here.

Table 1: Recent updates in photo-catalysts with different morphology and photocatalytic efficiency

Catalyst	Morphology	Synthesis method	Source of irradiation	H ₂ generation rate	Ref.
Ag/TiO ₂ , Hg	nanoparticle	sol-gel	Vapor lamp (365 Nm)	910 mmol g ⁻¹ h ⁻¹	48
Ni/TiO ₂ , Pyrex	nanosheets	solid state reaction	F lamp, 100 W (365 Nm)	26,000 mmol g ⁻¹ h ⁻¹	49
Fe ³⁺ ions doped and Ag deposited TiO ₂	nanoparticle	solvothermal	UV light Source	515.45 μmol/h/g	50
Fe/ TiO ₂	Na	anodization	xe arc lamp	174.30 mmol g ⁻¹ h ⁻¹	51
Cu/ TiO ₂	nanotubes	anodization	300 W, xenon, lamp	28,700 mmol g ⁻¹ h ⁻¹	50
Au/ TiO ₂	Na	anodization	300 W, xe lamp	3550 mmol g ⁻¹ h ⁻¹	52
Cu/ TiO ₂	nanoparticle	commercial tio ₂	125 W, Mercury Vapour lamp (High Pressure)	01–07 μmol/min	53
Pt or Au/TiO ₂	nanotubes	anodization	Xe/Hg lamp (High Pressure)	.06 μmol/cm ² /h	54
Au/Ti _{0.9} O ₂	nanosheets	solid state reaction	xe lamp 300 W	6753.00 μmol/h/g	55
TiO ₂ /WO ₃ /Au	Na	electrospinning	Xe Arc lamp, 300 W	270 μmol/h	52
rutile TiO ₂	nanosheet	solvothermal	300 W, xenon lamp	22 mmol/g/h (5 h)	56
N/TiO ₂ , PdO & Pt loaded NTiO ₂	nanoparticle	sol-gel	400 W, mercury lamp	55.0, 544.0, 772.0 μmol/h/g	48
SMK-TiO ₂	nanoparticle	sol-gel	150 W Mercury lamp (Medium Pressure)	3.3 mmol/240 min	57
Co-moderated TiO ₂	nanoparticle	commercial TiO ₂	300 W, Xenon lamp	Nanoparticle	58
Ag-Fe/TiO ₂	nanotubes Ti sheet (> 99% purity)	electrochemical	Xenon Lamp & Hg Llamp	Nanotubes Ti Sheet (> 99% Purity)	53
Cu(OH) ₂ /TiO ₂	nanotube arrays	electrochemical anodization	300W, Xe lamp	Nanotube Arrays	59

Advancement In Photo-Catalyst Developments

As per characteristics of elements throughout periodic table, a good number of semiconductors

have shown the capability for photo-catalytic water splitting to produce hydrogen. The requirements for a photocatalyst to be viable on large scale usage

involves high quantum yield; being inexpensive, earthly abundance, recyclable, nontoxicity, resistant to corrosion, and photo-stable; and also must have a long lifetime.³⁶ TiO₂, since Fujishima and Hondas study at 1972, has been regarded amongst the most preferable photo-catalysts for splitting water for its conveniences, e.g. being abundant, inexpensive, noncorrosive, photo-stable, and environmentally friendly.¹⁴ Nevertheless, TiO₂ can use only UV light for H₂ evolution for its vast band-gap energy of 3.2 eV, separated electrons and holes in VB and CB of TiO₂ can swiftly recombine and release energy or useless photons that barricade its practical utilization for Photocatalytic H₂ generation using solar energy.³⁷ Solar energy utilization basically depends on the electromagnetic wavelength of radiation in which photocatalyst shows activeness. Within 400 nm, the conversion efficiency of solar energy does not reach beyond 2%.³⁸ Efficiency improves to 16% and 32% if the spectral wavelength reaches 600 and 800 nm respectively. Oxides other than TiO₂, e.g. Cu₂O, WO₃, Fe₂O₃, and BiVO₄, were also examined for photocatalytic H₂ production, but their photo-catalytic efficiency for hydrogen evolution is still restricted by small amount of light-harvesting, large electron-hole recombination rates, and poor transportation of charge.³⁹ In times of BiVO₄, its edge position is inconvenient for HER. For Cu₂O, the efficiency solar to energy conversion is 18.0% theoretically, and it is vulnerable to auto-reduction in aqueous medium.⁴⁰ That's why it is very important to develop new photocatalysts to use the visible range and near IR region wavelength. Metal-free and Earth-rich catalysts such as g-C₃N₄, graphene, oxide of graphene, carbon nano-tubes have been examined greatly owing to its possible cost minimization in the time of scaling up.⁴¹ In recent times g-C₃N₄ based materials free from metal have gained popularity for application in splitting of water.⁴² However, the catalyst g-C₃N₄ still suffering from many drawbacks, for instance insufficient surface morphology, reduced conductivity & large recombination rate.⁴³ Another significant catalyst named metal-organic frameworks or MOFs are excellent photo catalyst for photo catalytic H₂ generation.⁴⁴ MOFs are composed of inorganic ions and organic substrate, which function as linking point & as connectors, correspondingly.⁴⁵ At last Researcher heed their concentration on catalyst development by implementing different technique such as Doping, Nanostructure, Heterojunction, Dye sensitization, Formation of Solid Solutions,

Sensitization with noble metal and Increasing Photo catalytically Active area etc.⁴⁶ Amid all of the technique applied Doping and Heterojunction is more striking.. Table 01 gives the recent update on catalysts with various morphology & photocatalytic H₂ production efficiency.⁴⁷

Material (Catalyst) Development techniques

Most decisive characteristic of a photocatalyst are: its optimum band gap, surface morphology, crystal structure and stability under light irradiation.. TiO₂ based photocatalyst or Anatase TiO₂ is the photocatalyst mostly subjected to modification techniques to enhance H₂ production. Other oxides, e.g. g-C₃N₄, Cu₂O, WO₃, Fe₂O₃, and BiVO₄, were also studied for photo-catalytic H₂ production, rather their performance or efficiency for photocatalytic H₂ evolution is evaluated by some factors like, light harvesting time and rate, charge recombination, band edge and low charge transportation.⁶⁰ Also, catalysts such as g-C₃N₄, oxides of graphene, graphene, nanotubes, and CDQs have been extensively investigated to develop their properties as they can exhibit better efficiency.⁶¹ Scientists are trying to develop the catalytic activity of photocatalysts through several techniques. Some of these are

Catalyst Development techniques

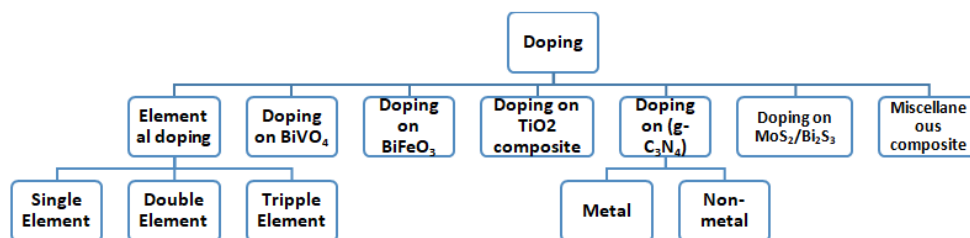
- Doping
- Heterojunction
- Dye sensitization
- Sensitization with noble metal loading
- Increasing Photo catalytically Active Area
- Modification of surface
- Nanostructure
- modification with Co-catalysts,

Doping

Among all of the stable and effective techniques for the development of catalysts, doping is the most effective and widely applied way to gear up catalyst's electronic activity as well as to accelerate the reaction surface. Non-metals and metals deposition onto the semiconductor surface enables supplying maximum active sites excellently for photo-catalytic hydrogen production. Besides, proper control of homogeneous distribution and metals particle size can supply sufficient active site resulting in maximum light transmittance.⁴⁵ Catalyst modification induces

more charges due to the reduction of band gap, hence exciting more electrons for the production of hydrogen.⁶¹ TiO₂ is one of the prominent and pioneer catalyst with maximum efficiency from 1972 to now.

Here, metal and non-metal doping of TiO₂, elemental doping on titanium-based catalyst, doping on the various composite catalyst, such as g-C₃N₄, BiVO₄, MoS₂/Bi₂S₃, BiFeO₃ are discussed in a brief.



Doping

Elemental Doping

Doping deals with the replacement of an anion or cation within the surface of a substrate with some other agents (element) (Fig. 2a). Only an element of a similar charge and radius can be placed into a cation. The doping technique affects the band structure and decreases the band-gap by introducing

a new forbidden level in the band. To choose the metal, its radius must match with the radius of the ion to be replaced. For example, in SrTiO₃ base lattice, Ti⁴⁺ (0.0605 nm) will be replaced by Ta⁵⁺ (0.064 nm) and Cr³⁺ (0.0615 nm) ions where F (0.133 nm) atom will replace by O₂ (0.140 nm).⁶²

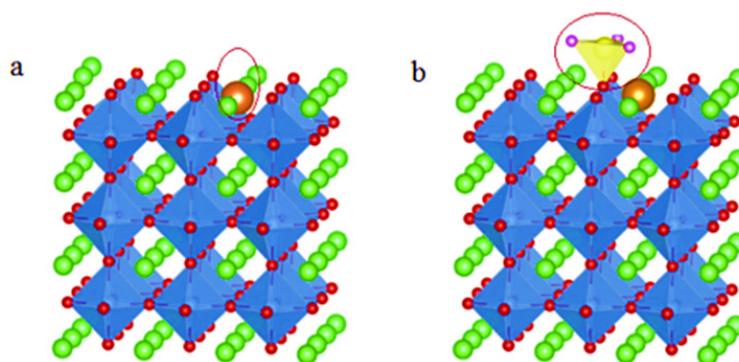


Fig. 2 : A 3-Dimensional representation for elemental doping on SrTiO₃⁶²

Doping with Single Element

Single-element doping is the replacement of single sites with one similar type of foreign element (fig. 2a). Although the sites are normally cation sites in the perovskite structure, such as A & B, but most replacement occurs at B site (fig. 2b). Different effects on PEC materials will occur for each doping entity because of the difference in the arrangements of valence shell electrons. Primarily, new donors or acceptors cause to form by doping in the forbidden band, resulting in the reduction in band gap. Currently, Cu doped CaTiO₃ shows an excellent result in H₂ production with a rate of 1447.8 mmol h⁻¹

under irradiation of UV light.⁶³ Here, table 02 exhibits the expected improved data obtained from photo catalyst while doping with a different single atoms with variable parameters. Results incur that the CaTiO₃ doping with Cu shows highest H₂ evolution rate of 1447.8 mmol h⁻¹ with UV light.⁶⁴ According to Shen P *et al.* SrTiO₃ catalyst, synthesized by polymerization method yield 47.00 mmol h⁻¹ H₂ evolution rate under λ>420.0 nm & λ<800.0 nm light irradiation while doping with Rh metal atom.⁶⁴ On the other hand according to the study of Sun X *et al.* Sr₂TiO₄ exhibit maximum hydrogen evolution i.e. 97.7 mmol h⁻¹ when doping with Cr under light

irradiation of ($\lambda > 250$ nm, visible).⁶⁵ They developed this catalyst with Solid-state reactions mechanism and found highest output. Zou J-P *et al.*, Yu H *et al.* get a regular output from SrTiO₃ catalyst while doping with Zn and Cr respectively under UV light irradiation.^{66, 67} They synthesized the catalyst

matrix in Sol-gel method. However, a significant result was found by Zhang H *et al.* from the catalyst Ti_{0.98}Cu_{0.02}O₃ by Ca doping system under UV light irradiation. Zhang H *et al.* found that 1447.8 mmol h⁻¹ hydrogen evolution from catalyst while doping with Ca with Sol-gel method.⁶⁴

Table 2: Outcome of doping with single element at perovskites (titanate-based) structure

Results obtained by single-element doping to titanate-based perovskites						
No	Catalyst	Dopants	Method	Light source	H ₂ generation rate	Ref.
1	SrTiO ₃	Rh	polymerizable complex,	UV lamp	47.00 mmol h ⁻¹	63
2	Ti _{0.98} Cu _{0.02} O ₃	Ca	sol-gel	UV lamp	1447.80 mmol h ⁻¹	65
3	Sr ₂ TiO ₄	Cr	solid-state reactions	visible	97.70 mmol h ⁻¹	66
4	Ba _{5/6/6} TiO ₃	Zn	sol-gel	UV lamp	2.90 mmol h ⁻¹	66
5	Sr _{2/3} TiO ₃	Zn _{1/3}	sol-gel	UV lamp	12.10 mmol h ⁻¹	64
6	SrTiO ₃	Cr	hydrothermal	visible and UV lamp	9.30 mmol g ⁻¹ h ⁻¹	67

Doping with Double Element

Here, replacement in the host material cause to happen with two types of foreign substrate at the same sites (B) or separate sites like X sites and A, B. Below in table 03, few effective cases listed through doping with the double element, along with the used parameters in experiments are shown. For example, on doping of cation with two elements, Sun *et al.* reported the increased hydrogen evolution rate to 211.4 mmol g⁻¹ h⁻¹ only with visible light ($\lambda > 415$ nm) in SrTiO₃, Ta⁵⁺ and Cr³⁺ at Ti⁴⁺ sites compared to 97.7 mmol h⁻¹ H₂ evolution rate for doping of SrTiO₃ with Cr. High improvement, above two-fold, in case of Ta addition.⁶⁵ Furthermore, the reported rate of H₂ evolution can be more accelerated if

UV light source is included. On Co-doping, diffuse reflectance spectra revealed that Cr/Ta ions form a 3d donor level of Cr³⁺, above O 2p valence band. Yu *et al.* reported similar results, as in table 3, Yu H *et al.* shows. A study shows that the rate of hydrogen evolution in a double element doped SrTiO₃ was more about twice than that of mono element doped SrTiO₃, while fabricated through the same method. For B 2p electron, top valence band position was around 0.38 eV.⁶⁷ But as Kang & Park reported the performance of composite catalyst material doped with double-element (15.4 mmol h⁻¹) was less than that of (Cr, Ta):SrTiO₃. (68). Results reveals that application of double doping in cation sites shows best outcomes than doping with only single element.

Table 3: Outcome of doping with double element at perovskites (titanate-based) structure

Outcomes of titanate-based perovskites listed through doping with double element						
No	Catalyst	Dopants	Method	Light source	Rate of H ₂ generation	Ref.
1	SrTiO ₃	Ta, Cr	spray pyrolysis	$\lambda > 415$ nm	211.4 mmol g ⁻¹ h ⁻¹	68
2	Sr _{0.9} Bi _{0.1} Ti _{0.9}	Fe _{0.1} O ₃	solid state	$\lambda > 250$ nm	185 mmol g ⁻¹ h ⁻¹	69
3	SrTiO ₃	B, Cr	hydrothermal	visible & UV	15.41 mmol g ⁻¹ h ⁻¹	67
4	CaTiO ₃	La, Ag	sol-gel with ultra-sonication	visible & UV	1064 mmol g ⁻¹ h ⁻¹	70
5	SrTiO ₃	Al, Au	solid state	visible & UV	348 mmol g ⁻¹ h ⁻¹	71

Doping with Triple Element

In doping with triple element, three dopant elements replace original host structure atoms, where two replace at A and B sites and the left other replaces O sites. Researchers doped anion to substitute O₂ sites with F for performing a research on material doped with double element in the same material as that used by Kang HW *et al.* in his work. Resultantly,

for maintaining balance in charge, rest elements changed their charge in the initial structure. For instance, in case of SrTiO₃:Cr/Ta, when F ions substitute O₂ ions Rh⁴⁺ & Ti⁴⁺ reduces Rh⁴⁺ respectively to Rh³⁺ & Ti³⁺ and it partially induces Rh³⁺ and Ti³⁺ formation, respectively from Rh⁴⁺ & T⁴⁺ in the sites B of the substrate, decreasing barrier towards the energy of activation and reducing stability.⁶⁸

Table 4: Outcome of doping with tri-element at perovskites (titanate-based) structure

Outcome of perovskites (titanate-based) listed through doping with tri-element						
No	Catalyst	Dopants	Fabrication Method	Wave Nature	Rate of H ₂ generation	Ref.
1	SrTiO ₃	F/Ta/Rh	spray pyrolysis	visible range	123.70 mmol g ⁻¹ h ⁻¹	71
2	SrTiO ₃	Ta/F Cr	spray pyrolysis	visible range	3887.5 mmol g ⁻¹ h ⁻¹	62

Here, charge distribution variation influences the band organization through making interactivity within electrons in a substrate. Also, F replacement in O₂ sites results in cation deficiency and cation deficiency are the root cause for the doping element to improve H₂ evolution in PEC. In a research by Kang HW *et al.* they noticed that catalyst SrTiO₃ yield 123.7 mmol g⁻¹ h⁻¹ H₂ while doping with tri-element such as (Rh/Ta/F). They synthesized the catalyst

with Spray pyrolysis method and the light irradiation was 4% under visible range. At the same time in a separate investigation, by Kang HW *et al.* registered that 3887.9 mmol g⁻¹ h⁻¹ hydrogen was evaluated from the SrTiO₃ catalyst while doping with Cr/Ta/F simultaneously. They also fabricate the catalyst matrix by spray pyrolysis method and conducted the reaction under visible light irradiation.⁷¹

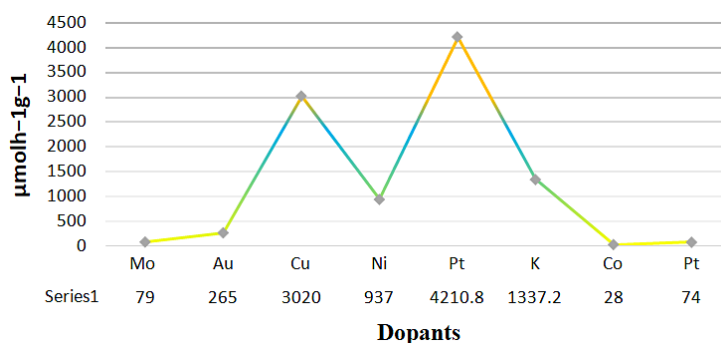


Fig. 3: Metal doping on g-C₃N₄ based photo

Doping on Photo-Catalysts based on Graphitic Carbon Nitride (G-C₃N₄)

Doping with Metal

Recently Graphitic carbon nitride(g-C₃N₄), drawn a considerable concern as well as effectively investigated just as green, viable photo catalyst which results in a convenience e.g. metal-free,

non-toxic semiconductor along with sensibility at the visible light range and narrow band gap , approximately, 2.7 eV.⁷² In addition, consisting with simple earth abundant element C & N, it is of low cost and also shows unique resistivity towards photo corrosion for the strength of covalent bonds shown by the atoms of carbon and nitride.⁷³

Also g-C₃N₄ shows exceptional photoluminescence (PL) characteristics, making it unstable as quality co-catalyst for other semiconductor catalysts.⁷⁴ But in practice, implementation of g-C₃N₄ as photo catalyst is limited, due to smaller specific surface area and high rate of recombination of photo induced charges.⁷⁵ Ultimately, Doping is one of the effectual initiative for adjusting electronic formations of g-C₃N₄ and to stimulate the reaction surface to escalate photo-catalytic activity owing to the work function and Surface Plasmon Resonance effect according to the previous writings.⁷⁶

In the year 2014, Zhong Y *et al.* conduct Pt doping on photo-catalysts based on Graphitic carbon nitride (g-C₃N₄), under light irradiation of (300 W Xe lamp, λ >420 nm) in Quartz reactor. They get hydrogen flow rate of 41.7 μmolh⁻¹g⁻¹ which was not significant to continue further work. Further in 2015 prominent

researcher Huang Z *et al* and Ma L *et al.* again doped g-C₃N₄ photo catalyst with Pt. The final product was then led for photoreaction under light irradiation of 300 W Xe lamp, λ >420 nm in Quartz reactor and Pyrex reactor respectively.^{77,78} Ma L *et al.* found 89.28 μmolh⁻¹g⁻¹ hydrogen production rate while Huang Z *et al.* found 261.8 μmolh⁻¹g⁻¹ in Quartz reactor. In 2018, Wang Y *et al* doped potassium (K) on Graphitic carbon nitride (g-C₃N₄) based photo-catalysts. They found that, in Pyrex reactor under light irradiation condition of 300 W Xe lamp, λ ¼ 400 nm, K doped g-C₃N₄ produce maximum 1337.2 μmol hydrogen at one hour.⁷⁹ In the same year, another study of Liu M *et al.* shows maximum 4210.8 μmolh⁻¹g⁻¹ efficiency of Graphitic carbon nitride (g-C₃N₄) based ,while doping with platinum (Pt).⁸⁰ But in 2019, Chen D *et al.* found 79.00 μmol hydrogen by Mo doping on Graphitic carbon nitride (g-C₃N₄) based photo-catalyst.⁸¹

Table 5: Metal doped photo-catalysts based on g-C₃N₄ for H₂ production

Year	Photocatalyst	Dopant (metal)	Reactor	Light Source	Efficiency μmolh ⁻¹ g ⁻¹	Ref.
2019	g-C ₃ N ₄	Mo	Pyrex reactor(P)	Xe lamp, 300 W	790.0	81
2018	g-C ₃ N ₄	Au	Pyrex reactor(P)	Xe lamp, 300 W	265.00	82
2018	g-C ₃ N ₄	Cu	Pyrex reactor(P)	Xe lamp, 300 W, λ >430 nm	3020.00	83
2018	g-C ₃ N ₄	Ni	Quartz reactor (Q)	Xe lamp, 300 W, λ >430 nm	529.10	84
2018	g-C ₃ N ₄	Ni-P	Pyrex reactor(P)	Xe lamp, 350 W	937.00	85
2018	g-C ₃ N ₄	Pt	Pyrex reactor (P)	Xe lamp, 350 W	4210.80	80
2018	g-C ₃ N ₄	K	Pyrex reactor (P)	Xe lamp, 300 W λ ¼ 420 nm	1337.20	79
2017	g-C ₃ N ₄	Co	Pyrex reactor(P)	Xe lamp, 300 W, λ > 420 nm	280.00	86
2017	g-C ₃ N ₄	Pt	Pyrex reactor(P)	Xe lamp, 300 W, λ ¼ 400 nm	740.00	87
2015	g-C ₃ N ₄	Pt	Quartz reactor(Q)	Xe lamp, 300 W, λ >420 nm	262.00	88
2015	g-C ₃ N ₄	Pt	Pyrex reactor (P)	Xe lamp, 300 W λ >400 nm	890.20	78
2014	g-C ₃ N ₄	Pt	Quartz reactor (Q)	300 W, Xe lamp, λ >420 nm	420.00	77

Non-Metal Doping

Besides metal doping, doping with non-metals can effectively increase semiconductor's photo-activity. In the modification of g-C₃N₄ polymers, doping with O, S, B & N; (the non-metal elements) shows excellent result while comparing with others. Its optical & electronic nature were effectively optimized for promoting photo-catalytic activity as a result of improved optical absorption process along with increased charge mobility. Hydrogen gas evolution performance should be enhanced as loading of various type of non-metal element that

tunes the catalyst formation by reducing the band gap, inhibiting electron-hole pair recombination rate and stabilizing the catalyst. Zhou *et al.*, during 2016, reported near 3.3 time's higher hydrogen production than undoped g-C₃N₄ over modified N-doped g-C₃N₄ photo-catalyst (CN-20) with maximum reported hydrogen production was 64 mmol h⁻¹ (Fig. 6(a)).⁸⁹ CN-20 catalyst was also documented for stability, as there was no notable decrease in the hydrogen production rate on repeated experiment under similar experimental situation used for four cycles (24 h), as Fig.6(b) reveals.

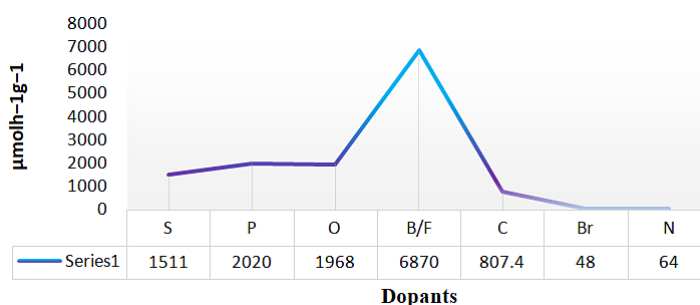


Fig. 4: Non-metal doping on g-C₃N₄ based photocatalyst

Table 6: The recent study of Non-metal loading on photocatalyst based on g-C₃N₄ for hydrogen generation

Year	Photocatalyst	Dopant (inorganic)	Reactor	Light Source	Efficiency μmolh ⁻¹ g ⁻¹	Ref.
2019	g-C ₃ N ₄	S	Pyrex reactor (P)	Xe lamp, 300 W, λ = 420	1511.2	92
2019	g-C ₃ N ₄	P	Pyrex reactor(P)	350 W, Xe arc lamp, λ > 420 nm	2020	93
2018	g-C ₃ N ₄	O	Pyrex reactor(P)	300 W, Xelamp λ = 420	1968.00	94
2018	g-C ₃ N ₄	B/F	Pyrex reactor(P)	Xe lamp, 300 W, λ > 420 nm	6870.00	95
2018	g-C ₃ N ₄	S	Pyrex reactor(P)	Xe lamp, 300 W, λ > 420 nm	240.1	84
2018	g-C ₃ N ₄	O	Pyrex reactor(P)	Xe lamp, 350 W,	1968.00	94
2017	g-C ₃ N ₄	P	Pyrex reactor(P)	Xe lamp, 300 W, λ > 420 nm	570.00	94
2017	g-C ₃ N ₄	C	Pyrex reactor(P)	Xe lamp, 300 W, λ > 420 nm	807.40	96
2016,	g-C ₃ N ₄	Br	Pyrex reactor(P)	Xe lamp, 300 W, λ ¼ 400 nm	480.0	91
2016	g-C ₃ N ₄	N	Quartz reactor(Q)	Xe lamp, 300 W, λ > 420 nm	640.0	89
2015	g-C ₃ N ₄	C	Pyrex reactor(P)	Xe arc lamp, 350 W, λ > 420 nm	540.0	97
2014	g-C ₃ N ₄	C	Pyrex reactor(P)	Xe lamp ,Visible light, λ > 420 nm	700.0	98

In another study by Chen *et al.* reported the 12 times higher enhanced photo-catalytic performance for sulfur loading than pristine g-C₃N₄ and long term stability for the water-splitting process, as it is documented in Fig. 6(c). This one resolved that S loading is able to efficaciously enhance the specific surface area, persuade the formation of nitrogen vacancy, retard photo produced electron-

hole pair recombination rate and improve the visible range responsiveness of the catalyst.⁹⁰ Similarly specified the non-metal Br doped g-C₃N₄, was also appeared having long-term stableness on visible range photo-catalytic activity for 20 h with highest hydrogen generation rate of around 48 mmol h⁻¹ as in the Fig. 6(d) showed. They also suggested that, the mechanism of reaction for water splitting using

photo catalyst designed for CNBr as demonstrated in the Fig. 6(e).⁹¹ Here, Table 7 demonstrates the cases for the non-metal doping on g-C₃N₄ aimed at water splitting using photo catalyst.

Doping on BiVO₄ based Photo-catalysts:BiVO₄

Centenary of semiconductors are used for their Photo catalytic Properties, because it is impossible to fulfill all the conditions of photo catalytic water splitting by a particular element. Accordingly, element improvement stands the significant note for improving Photo catalytic water splitting act. In recent time, BiVO₄ takes excessive consideration as photo-anode substances for PEC water splitting, since certain modified BiVO₄ photo-anodes fulfill several essential necessities enlisted above.⁹⁹⁻¹⁰¹ BiVO₄ is a n-type semiconductor photo catalyst with the maximum band gap energy of 2.4eV. Here, BiVO₄ engrosses sufficient amount of visible light spectrum and used as a stable, neutral, nontoxic, comparatively low-cost electrolyte.¹⁰²⁻¹⁰⁴ In comparison with other common O₂ evolution photo catalyst like Fe₂O₃ and WO₃, BiVO₄ consumes

a quite high CB (conduction band) energy (0.02 V vs. RHE). Therefore, the needless bias potential to elevate the photoelectrons upper the water reduction potential (0.0 V vs. RHE). However, the drawback is a very poor electrical conductivity with drippy water oxidation kinetics. Hence, several improvement techniques had undertaken for takeover the shortcomings of the BiVO₄ catalyst as a photo-anode and to magnify its photo catalytic water splitting properties. Doping is one of the significant steps of them. Bismuth vanadate is suffering from the problems of the transfer of electron. Therefore, doping in BiVO₄ can be a noble strategy to develop the electron transfer process in it and later photocurrent along with catalytic execution. In a research by Patil *et al.* informed that 2.00% of silver which is doping in uncontaminated BVO could rise its photocurrent density near about 3-fold as linked to an undoped BVO. In another work, Fang and his team presented that, the pure BVO Catalyst have less photocurrent density rather than Ag-BiVO₄ structure.¹⁰⁵

Table 7: The recent study of doping on BiVO₄ composite photo-catalyst

Year	Photo catalyst	Dopant (metal)	Reactor Solution	Light Source	Efficiency $\mu\text{molh}^{-1}\text{cm}^{-2}\text{h}^{-1}$	Ref.
2018	BiVO ₄	Nb-TiO ₂	1.0M KCl at P ^H 9.2	AM1.5G illumination	80 $\mu\text{molh}^{-1}\text{cm}^{-2}\text{h}^{-1}$	109
2018	BiVO ₄	Bi ₂ S ₃	Na ₂ S/Na ₂ SO ₃	1000 W m ⁻² (1 Sun).	417 $\mu\text{molh}^{-1}\text{cm}^{-2}\text{h}^{-1}$	106
2018	BiVO ₄	Nb-TiO ₂ /W	0.50 M phosphate buffer	AM1.50G illumination	80 $\mu\text{molh}^{-1}\text{cm}^{-2}\text{h}^{-1}$	110
2017	BiVO ₄	MDH	0.50 M phosphate buffer	AM1.50 G illumination	21 $\mu\text{molh}^{-1}\text{cm}^{-2}\text{h}^{-1}$	111
2017	BiVO ₄	3-Fe ₂ O ₃	phosphate buffer solution	AM1.50 G illumination	27.34 $\mu\text{molh}^{-1}\text{cm}^{-2}\text{h}^{-1}$	112
2016	BiVO ₄	CDs	0.50 M phosphate buffer	300.0 W Xe-lamp	0.92 $\mu\text{molh}^{-1}\text{cm}^{-2}\text{h}^{-1}$	107
2016	BiVO ₄	HDP	1.0M KCl at pH	1.0 G sun illumination	121 $\mu\text{molh}^{-1}\text{cm}^{-2}\text{h}^{-1}$	107
2016	BiVO ₄	WO ₃ -NRs	potassium phosphate (pH =7)	solar light, AM 1.50 G	102 $\mu\text{molh}^{-1}\text{cm}^{-2}\text{h}^{-1}$	105
2014	BiVO ₄	WO ₃ / (W; Mo)	0.5M K ₂ SO ₄ (pH 7.0)	100mWcm ⁻² , AM 1.50 G,	75 $\mu\text{molh}^{-1}\text{cm}^{-2}\text{h}^{-1}$	105
2011	BiVO ₄	RhO ₂ /Mo	-	AM1.50 G solar light	9 $\mu\text{molh}^{-1}\text{cm}^{-2}\text{h}^{-1}$	113
2011	BiVO ₄	Mo	seawater	simulated AM 1.50 G sunlight	7 $\mu\text{molh}^{-1}\text{cm}^{-2}\text{h}^{-1}$	113

Where Martin Rohloff *et al.* described that the photo catalytic water splitting routine of the Mo-doped BiVO₄ film photo-anodes are much better compared

to their pure BiVO₄. The photocurrent densities for Mo-BVO go to 1.90 mA cm⁻² at 1.23V vs. RHE under solar light irradiation (100.00mW cm⁻²).

In a work, Diane K. Zhong *et al.* described that the photo-current densities of BiVO₄, after W doping were improved to 0.7 mA cm⁻² at 1.23 V vs. RHE under 1.0 sun light illumination (100.00mW cm⁻²).¹⁰⁶ Amongst surface modification techniques deposition of catalysts layers on the BiVO₄ surface, cobalt phosphate (Co-Pi) displayed the significant benefits of being effortlessly coconspirator with the BiVO₄ surface. The Co-Pi alteration is a modest and

effective technique to produce an earth abundant water-oxidation electro-catalyst for developing photocatalytic water oxidation.¹⁰⁷ The modification of surface of BiVO₄ semiconductor with W-doped and Mo-doped, are increased the photocurrent densities to 1.25 and 4.6 mA cm⁻² at 1.23 V vs. RHE under illumination of 1.0 sun light, respectively.^{103, 108} Heretable 07 shows the recent study of doping on BiVO₄ composite photo catalyst.

Table 8: Key findings in development of Photocatalytic activity of BiFeO₃ by doping with Gd³⁺.¹¹⁴

Sl. No.	Catalyst	Doped Element	Preparation Method	Efficiency	Ref.
01	BiFeO ₃	nil	sol-gel synthesis	21.9 μmolcm ⁻² h ⁻¹	Yuxuan Yang, <i>et. al.</i> , 2018
02	BiFeO ₃	Gd ³⁺	sol-gel synthesis	67.6 μmolcm ⁻² h ⁻¹	Yuxuan Yang, <i>et. al.</i> , 2018

Doping on BiFeO₃ based Photo-Catalysts: by Gd³⁺

In a work, Yuxuan Yang *et al.* reported that, sol-gel synthesis along with photo-catalytic H₂ evolution of BiFeO₃ and Gd³⁺ doped BiFeO₃. The results of this work exhibits increased photo-catalytic H₂ evolution due to Gd³⁺ doping. The H₂ production rates are about 21.90 and 67.60 μmol cm⁻²h⁻¹ for BiFeO₃ and Gd³⁺ doped BiFeO₃, respectively. So,

it is absolutely larger photocatalytic activity, the rate, more than three times of Gd³⁺ doped BiFeO₃ than that for pristine BiFeO₃. So, Gd³⁺ doping effects performance of BiFeO₃.¹¹⁴ Also, It is mentionable that for a particulate photo-catalyst the H₂ production ability depends on its different properties e.g. microstructure, crystallinity, electronic and optical etc.¹¹⁵

Table 9: The recent study of Doping on TiO₂ & TiO₂ based composite photocatalyst

Year	Photocatalyst	Dopant (metal)	Reactant	Light Source Solution	Efficiency μmolh ⁻¹ g ⁻¹	Ref.
2019	SrTiO3	Al	Pure water	300.0 W, Xe Lamp	05.70	118
2018	PCN-777	Pt	TEOA	300 W,	586.00	116
2018	RP/TiO2	Red-P	Methanol	350.0W, mercury Lamp	276.00	119
2006	Sr3Ti2O7	NiOx	Pure water	Hg lamp,400–450.0 W	144.00	120
2002	CaTiO3	NiOx	Pure water	Xe lamp,400–450.0 W	30.00	121
2002	Sr4Ti3O10	NiOx	Pure water	Xe lamp,400–450.0 W	170.00	122
1998	B/Ti oxide	Pt	Pure water	Hg lamp,400–450.0 W	22.00	123
1997	K2La2Ti3O10	NiOx	Pure water	Hg lamp,400–450.0 W	2186.00	124
1997	TiO2	Pt	Pure water	Xe lamp,400–450.0 W	568.00	125
1995	TiO2	Pt	Pure water	Hg lamp,400–450.0 W	106.00	126
1987	TiO2	NiOx	Pure water	Hg lamp,400–450.0 W	62.00	127
1985	TiO2	Rh	Pure water	Xe Lamp, 400–450.0 W	449.00	128
1980	SrTiO3	Rh	Pure water	Hg lamp, 400–450.0 W	27.00	129, 130
1980	SrTiO3	NiOx	Pure water	Hg lamp, 400–450.0 W	40.00	127, 131

Doping On TiO₂ & TiO₂ Composite Photo-Catalyst

TiO₂ & TiO₂ composite photocatalyst is the best, efficient, and cost-effective catalyst for photocatalytic water splitting. Since 1972 enormous scientists or researchers work on it. The TiO₂ & TiO₂ composite photocatalyst could be further stabilized by the deposition of various metal and non-metal elements on its surface to increase catalytic activity. According to Hang Liu *et al.* the photocatalyst Pt/PCN-777 exhibits excellent H₂ production rate of 586 mmolcm⁻² h⁻¹ in the presence of the TEOA reagent as a sacrificial agent under 300.0 W xenon lamp.¹¹⁶ The most important is that, this composite is recyclable under the normal catalytic conditions. A prominent researcher Y. Goto *et al.* processed a TiO₂/CoOOH/RhCrOx/SrTiO₃:Al photocatalyst into a 5.0 *5.0 cm sheets & the sustainability of the substance was tested by a panel-type photo reactor with water depth 1.5 mm by simulated light and ambient pressure.¹¹⁷ The water splitting rate of these sheets are 5.7 μmolh⁻¹g⁻¹ and H₂ generation efficiency is 0.4% at the initial duration of irradiation.

Where according to Hao Lyu *et al* the AQY of the resulting RhCrOx/SrTiO₃: Al at the time of overall water splintering was measured to be 54.0% at 360.00 nm, which consistent with the ancestral work.¹¹⁸

Doping (Copper) on MoS₂/Bi₂S₃ Photocatalyst

In a study, W. P. Cathie Lee fabricated a flower-like Copper-doped molybdenum disulfide/bismuth sulfide (Cu-MoS₂/Bi₂S₃) photo-catalyst. The sample photocatalysts with differing quantity of Cu were utilized in the photo-catalytic water splitting for H₂ production under simulated sunlight irradiation. The photocatalysts demonstrated high Photocatalytic activity with a most favorable Cu loading of 20.0mol%, reaching a total hydrogen evolution of 32.4 mmol/h on reaction for 6 hours(Fig:-5.0). The Copper doped samples showed increased performance rising about 1.4 times of non-doped samples. The reaction time taken by the different samples are also shown in (Fig: 5-2) respectively.¹³²

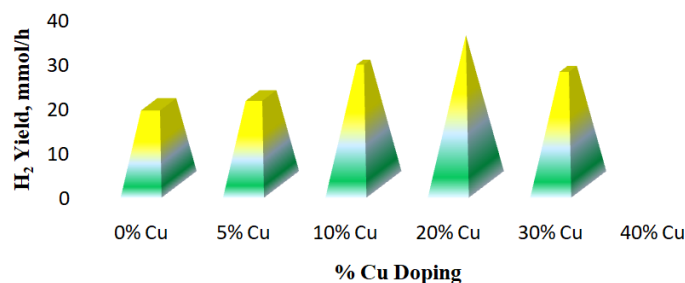


Fig. 5: Variation of Hydrogen production rate from variable Cu doping on Na₂S/Na₂SO₃ mixture illuminated under simulated sunlight over the duration of 6.0 h

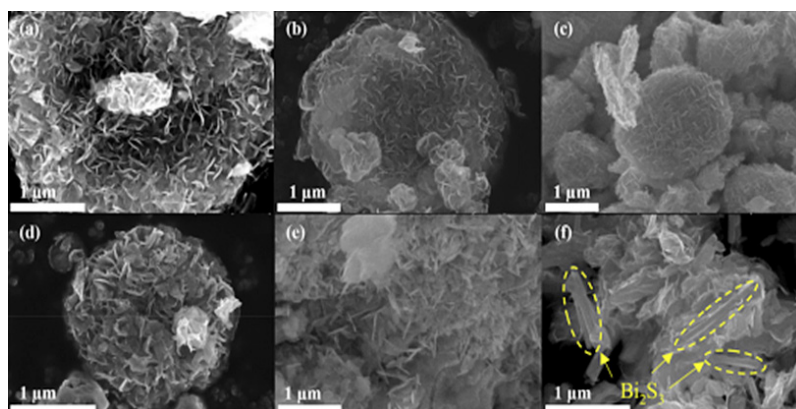


Fig. 6: Some images from FE-SEM of MoS₂/Bi₂S₃, (a) Undoped (b) 5.0mol% (c) 10.0mol% (d) 20.0mol% (e) 30.0mol% (f) 40.0mol%¹³²

The crystal structure and surface morphology info of synthesized photo-catalyst were inspected by W. P. Cathie Lee using TEM and FE-SEM.¹³² The standard structure of non-doped MoS₂/B₂S₃ is demonstrated in Fig. 2(a), where MoS₂ have been seen to cover surface of Bi₂S₃, growing on it.¹³³ In each of six images, crumpled MoS₂ nano sheets is found to accumulate onto Bi₂S₃ surface, producing a flower-type frame.¹³⁴ Upon copper (Cu) doping MoS₂/Bi₂S₃, no notable alteration on samples surfaces were noticed (Fig. 2(b) & (c)). Still, at greater Copper loading to 20.0mol%, on the surface the grown MoS₂ sheets were larger enough to be visible and distinguishable (Fig. 2(d)).¹³² But on increasing Copper(Cu) to 40.0mol%, the distinct Bi₂S₃ discoid's not formed, rather some Bi₂S₃ noticed to be in rod form (indicated as yellow in Fig. 2(f)) where MoS₂ sheets were in a arbitrary form.¹³²

Doping on Miscellaneous Composite Photo-Catalyst

Deposition of a foreign particle onto the semiconductor surface can supply maximum active surface for excellent Photo-catalytic H₂ production. There are many more option with semiconducting properties for Photocatalytic water splitting. Among

them K₂La₂Ti₃O₁₀, possesses a perovskite structure is one of a unique catalyst photo catalysis.¹³⁵ H₂ evolving happens on NiOx co-catalyst where O₂ evolves from hydrated interlayer. Various niobate, titanate and tantalite photo-catalysts with perovskite structure been reported from the period of K₂La₂Ti₃O₁₀ photocatalyst was designed. Sr₃Ti₂O₇ and Sr₄Ti₃O₁₀ photo-catalysts have perovskite slabs of SrTiO₃. La₂Ti₂O₇, La₂Ti₂O₇:Ba, KLaZr_{0.3}Ti_{0.7}O₄ and La₄CaTi₅O₁₇ photocatalysts with perovskite structure which give a maximum quantum yield. Na₂Ti₆O₁₃ and BaTi₄O₉ with a holo-tube type structure is also a unique photo-catalysts. On the other side Catalyst KTiNbO₅ shows activity when it prepared through a polymerizable complex composite system. In a study by S. Ikeda *et al.* they found that K₂La₂Ti₃O₁₀ yield 2186µmol Hydrogen in 0.1M KOH solution.¹²⁴ They used NiOx as dopant and the irradiated light intensity was 400 to 450 W mercury lamp with quartz cell. On the other hand in the year 2006 get 2390µmol Hydrogen from a quartz cell using K₃Ta₃B₂O₁₂ as a catalyst and Pure water Reactant Solution. Table 10 shows a brief summary of recent study on miscellaneous catalyst for Photocatalytic water splitting process.¹³⁶

Table 10: Some study of doping on miscellaneous composite photo-catalyst

Year	Photocatalyst	Dopant (metal)	Reactant Solution	Light Source	Efficiency µmolh ⁻¹ g ⁻¹	Ref.
2008	LiCa2Ta3O10	NiOx	Pure water	Hg-Q lamp	59.00	136
2007	CeO2:Sr	RuO2	Pure water	Hg-Q lamp	110	122
2006	Na2Ta2O6	NiO	Pure water	Hg-Q lamp	391	137
2006	K3Ta3B2O12	None	Pure water	Hg-Q lamp	2390	138
2005	Cs2Nb4O11	NiOx	Pure water	Hg lamp, 400-450 W	1700	139
2005	NaCa2Nb3O10	RuO2	Pure water	Hg-Q lamp	118	140
2005	Sr5Ta4O15	NiO	Pure water	Hg-Q	1194	141
2005	Ba5Ta4O15	NiO	Pure water	Hg-Q	2080	120
2004	Y2Ti2O7	NiOx	Pure water	Hg lamp	850	142-144
2004	La3NbO7	NiOx	Pure water	Hg lamp, 400-450 W	35	142
2003	KaLaZr0.3Ti0.7O4	NiOx	Pure water	Hg lamp, 400-450 W	230	145
2000	K2PrTa5O15	NiO	Pure water	Hg-Q	1550	146
1997	Rb2La2Ti3O10	NiOx	0.1 M RbOH	Hg-Q	869	147
1997	K2La2Ti3O10	NiOx	0.1M KOH	Hg lamp, 400-450 W	2186	148
1996	KTaO3	Ni	Pure water	Hg-Q	60	148, 149

Heterojunction

The heterojunction is the interface that takes place between two layers or sectors of varying crystalline

semiconductors. These semiconducting materials have a different band gaps as contrary to a homo junction. Many reviews have shown that various

semiconductors can be coupled with BiVO_4 for favorable result. The formation of successful hetero junction has been reported between BiVO_4 and WO_3 ,¹⁵⁰⁻¹⁵² SnO_2 ,^{153, 154} Fe_2O_3 ,^{155, 156} CuWO_4 ,¹⁵⁷ and CdS ,^{158, 159} Kim *et al.* showed that hetero type dual photo-anodes, HDP, of BiVO_4 & $\alpha\text{-Fe}_2\text{O}_3$.¹⁵⁶ Reports also implies largely increased photocurrent on HDP of $\text{BiVO}_4/\alpha\text{Fe}_2\text{O}_3$ becoming permanent. 7 mAcm^{-2} photocurrent at 1.23V vs. RHE has been reported below 1 solar radiation making subsequent hydrogen production for $\text{BiVO}_4/\alpha\text{Fe}_2\text{O}_3$ nearly $80\mu\text{molcm}^{-1}\text{h}^{-1}$ by Savioet *et al.* On the other hand, the $\text{Fe}_2\text{O}_3/\text{BiVO}_4$ photo-anode containing 3 spin coated films demonstrated 1.63mAcm^{-2} photocurrent density at 1.23V vs. RHE, reported by Xia *et al.* that is nearly 2.2 times higher in comparison to pure BiVO_4 photo-anode, submerged in 0.1M KH_2PO_4 (pH 7) electrolytic solution beneath AM1.5G sun light.¹⁵⁵ Rates of hydrogen production for $\text{Fe}_2\text{O}_3/\text{BiVO}_4$ has been around $28\mu\text{molcm}^{-2}\text{h}^{-1}$, quite larger in comparison to BiVO_4 photo-anode. A $\text{BiVO}_4/\text{CuWO}_4$ heterojunction electrodes made by Pilli *et al.* via spray accumulation method was reported two times photocurrent density to pristine BVO at 1.0V vs. Ag/AgCl in 1.0M Na_2SO_4 electrolytic solution at pH 7.¹⁵⁷ In contrary to pristine BVO, $\text{BiVO}_4/\text{WO}_3$ largely enhanced the IPCE, Incidence of Photon to Current Efficiency, from 9.3% to 31% as reported by Grimes *et al.* referred it to the phenomenon of enhanced electron migration towards WO_3 from BiVO_4 .¹⁶⁰ Also, as reported by Savio *et al.*, BiVO_4 and ZnO pairing generate a significant, 2 mA/cm^2 at 1.23V vs. RHE, photocurrent density in observable radiation range.¹⁶¹ Similarly, four times amplified photo current of $\text{BiVO}_4/\text{TiO}_2$, pairing of BiVO_4 and TiO_2 , has been reported by Kimura *et al.*, contrary to pristine BiVO_4 on 100mWcm^{-2} brightness, and they ascribed it to the formational alterations of BiVO_4 which improved electron transferring throughout the junction.¹⁶²

Dye-Sensitization

For HOMO and LUMO states being reconfigurable on anchorage of various ligands, dye sensitization is considered an effective way to improve the visible range response of photocatalyst for hydrogen generation. Broad usage for dye sensitization is to set visible light to transform energy. Some of the dyes are possible to be utilized in solar cells and Photo-catalytic methods, which have redox property and which are sensitive to visible light.¹⁶³⁻¹⁶⁵

On illumination of visible light, electrons from excited dyes can be infused to the conduction band of semiconductors, causing inauguration of photo catalytic actions as described in Fig:- 7. Some dyes such as safranin O/EDTA, T/EDTA, are susceptible to take in visible light to generate reducing agents electrons which have enough strength to generate H_2 even without semiconductors.¹⁶⁶ But it is very little H_2 generation rate by dyes without semiconductors.¹⁶⁴ Dhanalakshmi *et al.* carried out a parametric research to study the effect of applying 2p as a dye sensitizer on Photocatalytic H_2 generation from H_2O , under visible light irradiation.¹⁶⁷

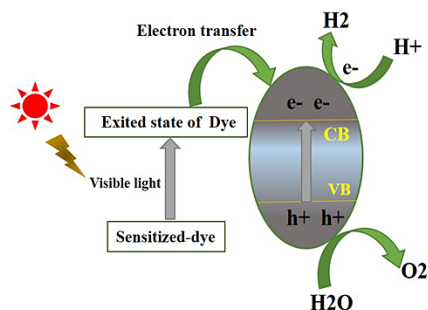


Fig. 7: Schematic representation of dye sensitizer action mechanism

Dhanalakshmi *et al.* observed improved H_2 generation rate under visible range radiation due to adsorption of dye molecules to the TiO_2 on parametric research studying the influence of applying 2p as a dye sensitizer on Photocatalyst based H_2 generation from H_2O . Splitting process.¹⁶³ Gurunathan *et al.* noticed influence of various dyes, for example, EDTA, during H_2 generation for SnO_2 photocatalyst using or not using sacrificial agents. Having band gap 3.5 eV and, SnO_2 was unable to be activated on visible irradiation.¹⁶⁸ On dye sensitization, SnO_2 was capable of H_2 generation on visible range irradiation. As observed, overall order of efficiency for dyes for improving rate of H_2 generation is as following: Eosin blue>Rose Bengal>Ru(bpy)₃²⁺>RhodamineB>Ac riflavin>Fluorescein.¹⁶⁷ By analyzing the physico-chemical properties of these dyes, a effective conclusion could be dawn.⁵²⁷ Like as Rhodamine pose a longer absorption range maxima including more negative potential (.545V) than conduction range (.34V) of SnO_2 (167). But the problem is that it does not improve the H_2 production rate significantly.

Table 11: Absorption wavelength maxima λ_{\max} (nm) dyes¹⁶⁹

Sl. No.	Dye	Class	λ_{\max} (nm)
01	Thionine (TH+)	Thiazin	596
02	Toluidine blue	Hiazin	630
03	Methylene blue (MB)	Thiazin	665
04	Eosin	Xanthen	514
05	Azure B	Thiazin	647
06	Azure A	Xanthen	535
07	Azure C	Thiazin	620
08	Phenosafranin (PSF)	Phenazin	520
09	Saf-O/SO	Phenazin	521
10	Saf-T/ST	Phenazin	524
11	Neutral red (NR)	Phenazin	534
12	Neutral red (NR)	Phenazin	534
13	Fluorescein	Xanthen	490
14	Erythrosin B	Xanthen	525
15	Dye	Xanthen	530

Sensitization with Noble Metal

Noble or precious metals, comprising Pt, Pd, Au, Ni, Rh, Cu & Ag, proved very efficient to improve photocatalytic activity of TiO_2 .^{170, 171} For these noble metals, Fermi levels are lesser in comparison to TiO_2 and another similar photocatalyst. The photogenerated electrons transfers towards metal particles from conducting band of photocatalyst, depositing, while holes stay on the Valance Band of the photocatalyst. This decreases the possible rebanding of electron and hole greatly, leading to effective separation and stronger photo-catalytic reaction.¹⁷² The prominent researcher Anpo & Takeuchi accustomed ESR, signals to observe transferring of an electron from photo-catalyst towards Pt. Increased Ti^{3+} signals were observed on increasing irradiation duration and Pt loading decreased the of Ti^{3+} quantity. This investigation shows electron shifting towards Pt particles from TiO_2 (Titanium dioxide). With electron deposition on particles, Fermi levels of the noble metals switch closer to the Conduction Band within TiO_2 photo-catalyst leading energy levels towards more negative(-ve) direction which is effectual for splitting water, producing H_2 .¹⁷³⁻¹⁷⁵ Small size metal particle accumulation cause huge shifting of Fermi level on negative (-ve) direction on surface of TiO_2 catalyt.¹⁷³ Electrons deposited on the metal particles

can move towards H^+ upon the surface, adsorbed, and subsequently reduce H^+ to form H_2 . Hence, noble metals having satisfactory work function able to assist in transferring electron, resulting in increased photo-catalytic activity.¹⁷⁶ Bamwenda *et al.* compared H_2 generation from water-ethanol solution using TiO_2 photo-catalyst loaded with two different metals, Au and Pt. they also examined variant methods for depositing metal particle, for example, deposition–precipitation, photo deposition & impregnation method.¹⁶⁷

They observed that Pt loaded TiO_2 better operated than Au loaded TiO_2 . On the other hand, Au loading arranged by photo deposition operated better among other methods. Changing could be attributed to improved contact in the photo deposition system between TiO_2 active sites and metal particles. But, the preparation system was hardly influencing in case of Pt-loaded TiO_2 .¹⁷⁷ Among others Sakthivel *et al.* observed good loading in experiment for photo oxidation of acid green 16 treatment with TiO_2 photocatalyst loaded with Pt, Au & Pd. As written above, photon absorption by TiO_2 can be hampered by too much deposition of metal particles and also it may lead to formation of centers for charge recombination, resulting in less efficiency.¹⁷⁷

Increasing Photo Catalytically Active Area

Photo catalytically active field in a photocatalyst is a necessary factor that readily impacts H_2 generation rates. So, it was a concern to apply methods for enhancing photo catalytically active area. Two ordinary but efficient ways exist for enhancing the specific surface area. The first way is building uniform nanoparticle-containing thick surfaces and incorporating second material (nanowires, nano cells, nanoparticles, etc.) covering primary photocatalyst exterior is the second way. CdS nanorods as well as nanowire highly active photocatalyst for hydrogen generation can be produced through solvothermal & hydrothermal methods. Also, ultrasonic mediating precipitation, two-step aqueous route, and some additional ways can be effectively used to synthesis mesoporous (CdS) Nanoparticle.⁴⁴

Modification of Surface with Graphene and other Carbonaceous Material

At present, Surface moderation of the photo-catalyst is performed with carbonaceous materials such as graphene, graphene quantum dot (GQD)s, carbon nano dots, carbon nanotubes (CNTs) and fullerenes (C_{60}) for improving H_2 generation in UV, UV-VM, and visible range area has drawn more remark because of the expanded visible-light absorption range and enhanced charge transfer.⁴⁴ Graphene exhibits excellent electron mobility ($200,000 \text{ cm}^2 \text{ V}^{-1} \text{ s}^{-1}$), substantial surface area specific ($2630 \text{ m}^2 \text{ g}^{-1}$), superior conductivity, electrical & thermal, and good chemical and physical stableness. Also, it is handily achievable from graphite bulk through mechanical, chemical, and thermal ways.^{178, 179} Zhang *et al.* pointed out the synthesis of grapheme /TiO₂Nano composites and the improved photo catalytic hydrogen production through splitting of water, as well as observed that the photo catalytic performance of grapheme /TiO₂ Nano composites rely on rGO ratio and calcination process.¹⁸⁰ In another work of Li *et al.*, graphene quantum dot (GQD)/ TiO₂ composite co-doped with sulfur and nitrogen (S,N-GQD/TiO₂ photocatalyst) showed much improved performance than pristine TiO₂ caused by improved visible radiation absorbance and efficient dissolution and transferring of photo generated charge.¹⁸¹ Fan *et al.* systematically conducted an inspection on reduction method influence on the hydrogen production performance of the Nano composite TiO₂/RGO, and observed that Nano

composite produced through hydrothermal method showed the best performance in H_2 generation activity on UV-Vis light radiation.¹⁸² Also, Fan *et al.* observed that grapheme quantum dot anchored TiO₂ showed improved photo catalytic hydrogen generation performance on using methanol solution because of graphene quantum dots (GQD) operating as effective reservoirs for electron and fantastic photo sensitizer's for Titanium dioxide.¹⁸³

Formation of Solid Solutions

A Solid solution production for compressing band-gap of semiconductors is a proper way to enhance efficiency for visible light absorption and utilization. Solid solution of ZnS and AgInS₂, (AgIn) $xZn_{2(1-x)}S_2$ consisting of a compressed band-gap exhibited high visible-light photo-catalytic hydrogen production activities from aqueous S^{2-} and SO_3^{2-} solutions for sacrificial purpose. On AgInS₂ ratio increment to ZnS, the light absorbance of (AgIn) $xZn_{2(1-x)}S_2$ solid solutions transferred to larger wavelengths because the photo-physical, photo-catalytic activities of (AgIn) $xZn_{2(1-x)}S_2$ solid solutions were dependent upon the structure changing for band position variation.⁴⁴ In addition, easily produced solid solutions from same crystal formation ZnS and CdS, ZnS-CdS photocatalyst are fantastically responsive towards visible-light for hydrogen generation.¹⁸⁴

Reactor Design & Development

A chemical reactor is an enclosed system in which chemical changes are takes place. The scheme/model of a chemical reactor deals with multiplex aspects of chemical engineering. Chemical engineers design a reactor to maximize the efficiency for the given reaction. Reactor modeling is a significant part in photo-catalytic water splitting systems as well as hydrogen production plants.

Factors to be consider for reactor design

- Geometrical set-up of the reactor
- Source of radiation (Natural or artificial)
- Catalyst (Slurry or hold in support)
- Sacrificial agents (CH_3OH , Waste Water, etc.)
- Light source position ($35 - 45^\circ$ angle, Concentric)
- Sacrificial agents
- Irradiation time
- Shelf-life

Photo-Reactor Design

The photo-reactor is any chamber or vessel where reaction between the photo-catalyst and reactants takes place with the presence of photon (light) and Sacrificial reagents (where needed). Different types of reactor based on UV and visible light irradiation has been shown in Fig: 8.²⁸ The photo-catalyst and light source are the main constituents of photo-reactor. For better photo-catalytic performance, an ideal photo-reactor must have uniform light distribution.¹⁸⁵ Tactics of operation and phase are important factors which determine the types of photo-reactor. Here Table-12 demonstrates the benefits and drawbacks of different photo-reactors. Table-12 summarized the benefits and drawbacks of different types of photo-reactor.

Batch-type Photo Reactor

The batch type reactor is the primary photo reactor in reactor types. Here Fig: 9.0 exhibits a batch type photo reactor for the catalytic hydrogen evolution from water. This types of the batch reactor are consist of a catalysts bed, reaction vessel, cooling water system, Quartz windows, light source, evacuation system, sample collection system, and gas detection device.^{28, 186} The water jacket around the reactor circulates water continuously to control the reactor and reaction temperature at a particular range. Light source will emit rays along the quartz windows.

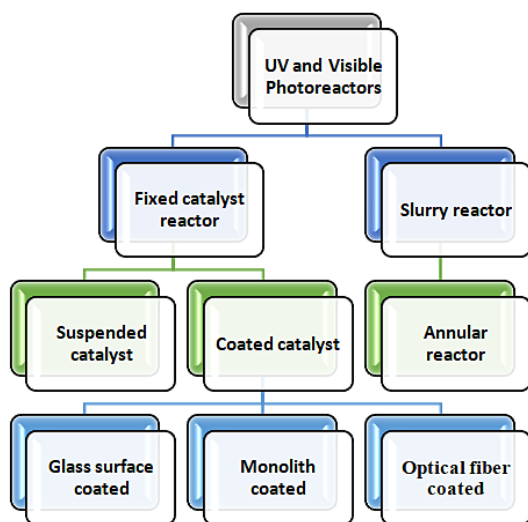


Fig.8: Types of photo-reactors for visible and UV light photo-catalytic to produce hydrogen²⁸

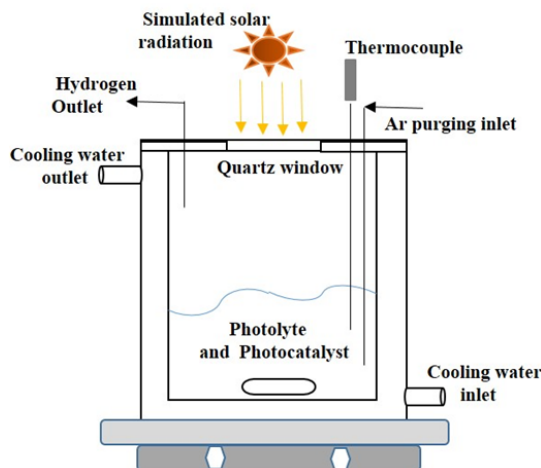


Fig. 9: Pictorial representation of a typical photo reactor built with stainless steel vessel and quartz oxide²⁸

Continuous Annular Photo-Reactors

Continuous annular photo-reactors are composed of a ring shaped reactor with a light source located in the center. The inert N₂ environment is maintained into the reactor, to isolate the system from the surroundings. A constant flow of Ar gas bubble is provided through the reaction slurry to keep the suspension homogeneous. To analyze, a portion of the produced hydrogen gas is inserted to a gas valve of gas chromatography (GC). The benefit of continuous annular photo-reactors is to enhance the liquid-gas interfacial area, which simplifies the release of H₂ from the photo-catalyst surface. One of the major drawbacks of these types of the reactor is, more photon can be received by the interior of the annular reactor than that of the exterior.

Photo Catalytic Membrane Reactor

Photo catalytic membrane reactor (PMRs) is effective for sustainable production of hydrogen by suppressing the reversed reaction between O₂ and H₂. Pure hydrogen can be obtained in a single step without further purification. In the case of PMRs design, photo-catalyst and metal loading, the mechanical resistance, permeability, membrane morphology are important factors to be considered and needed to get excellent efficiency of catalytic membrane system while in hydrogen evolution. There are various types of PMRs for hydrogen evolution, such as H-type Photo-catalytic

reactor (HPR), membrane electrode photo-catalyst assembly (MEPA), membrane twin reactor (MTR), and polymer membrane electrode assembly (PMEA).²⁸

Optical Fiber and Honeycomb Reactors

Generally Optical fibers, made of silica, are used to transmit light from one end to another end of the fibers. Light is split into two parts by the variation of refractive index between the quartz core and the semiconductor, such as TiO₂, coating during hitting the internal surface of the fiber.²⁸ Some portion of the light is transmitted and reflected through the fiber, while the rest fraction excites and penetrates the titanium layer on the interface. Thus, photo-reactions occur through the formation of electron-hole pair. As a result, optical fibers are utilized to radiate the light properly in the interior of a photo-reactor.¹⁸⁷ Light is passed through the fibers core by forming a cover which is lower refractive index that captures light beam in the core through total internal reflection.¹⁸⁸ Formerly, H₂ production rate was increased through photo catalytic water splitting using optical fiber coated with SiO₂ and TiO₂.¹⁸⁹ There are several benefits of optical fibers such as: It has higher efficiency enlighten the interior of reactor uniformly and it causes higher interactions between irradiations and catalyst surface.

Monolith Reactor

It is a multifunctional reactor which is integrated with separation and heat exchanger. The designs of a monolith reactor are uniform sets with a parallel line that can be constructed into various configurations (sizes and shapes). Application of monolith reactor having a narrow path with larger light beam interaction surface area (SA) can enhance the transformation and product rates.¹⁹⁰ Because of its excellent properties the Ceramic monolithic reactor formations shows an attractive choice to commonly designed catalyst nubbles or powders. Monoliths has several advantages over typical catalyst powders or nubbles, such as: improved weight transfer rate, good coating adhesion, better porosity, minimal pressure fall, better thermal and mechanical strength.¹⁹¹ Current improvement in photo (light) technology exhibited that, when compared with other commercial reactors, the monolith reactors have several benefits over them. In 2017, splitting of water for hydrogen evaluation with sacrificial agent, ethanol, in a monolith photo-reactor has been tested

by Gaudillere *et al.*¹⁹² According to Tahir *Met al.*, the quantum efficiency (QE) in micro-channel monolith reactor gave much higher (0.10%) than deal with cell type reactor (0.0005%).¹⁹³ In another analysis performed by Tahir *Met al.* they used/applied photo catalyst NiOeIn₂O₃/TiO₂ which showed superior performance in the batch type monolith photo reactor than considering cell type reactor under identical conditions of reaction with efficiency of 14.13 times higher.¹⁹⁴

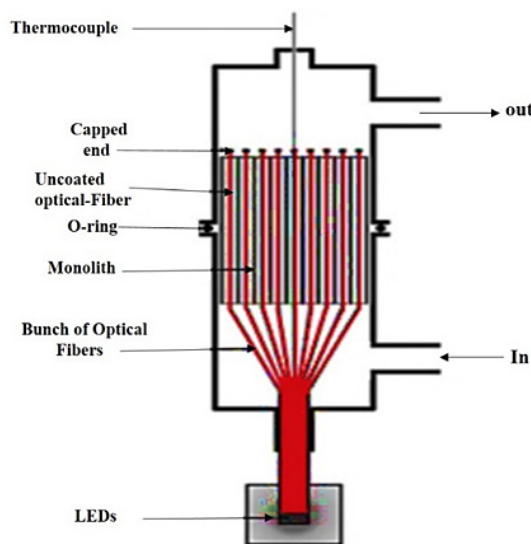


Fig. 10: The pictorial representation of an optical fiber honeycomb reactor¹⁸⁵

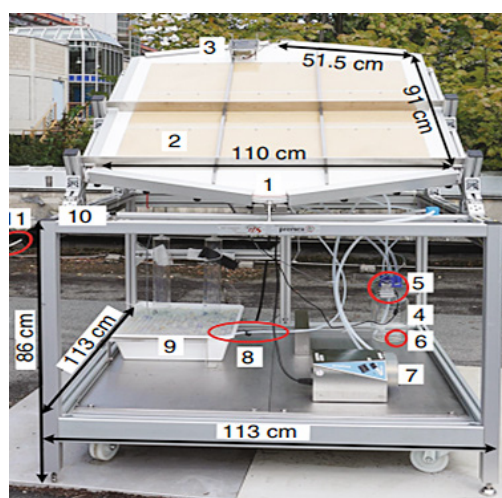


Fig. 11: The pictorial representation of a photo-reactor (large scale) for photo-catalytic reactions with an immobilized photo-catalyst¹⁸⁶

Particulate Photo Catalytic Reactor

Particulate photo catalyst reactor systems are narrated here having some facilities in case of designing cost and scale-up potential as compared with photo electrochemical and photovoltaic systems.¹⁹⁵ However, the development of photo catalytic water splitting set up even to the one to one meter scale has rarely been published, although the ultimate demand of fabricating plants tens of square kilometers.¹⁸⁶ Elsewhere, the power generation through photovoltaic system have been installed and commercialized in an extend phase. This indicates a non-stop challenge to the application of photo-catalytic splitting of water as a way of production of solar fuel.

Formerly, photo-catalytic water splitting has been studied in flask-type reactors using suspensions of photo-catalyst powders on the small-scale. Nevertheless, the disadvantage in the development of suspension systems can be guessed from the deficiency of big-scale displays of water splitting by sunlight overall with noticeable values of STH. Honestly, this an attempt is annoying on big scales

for various factors.¹⁸⁶ Firstly, it is challenging to lessen the costs of reactor, such as huge water is required. For example, 1 cm depth, water quantity in a reactor increases in values of 10 kg one square meter and reactors seem to be larger and high cost. This is not be feasible on a big scale production process assuming that the highest cost allowed for the complete hydrogen production systems is about US\$102 m⁻², as mentioned earlier.¹⁹⁶ Secondly, there is a tendency of the particulate photo-catalysts to precipitate to the basement of the reactor if not the reactor is positioned perfectly. They do not receive incident light effectively too. Tubular shaped reactors combined with a CPC (compound parabolic concentrator) have been experimented for big scale industrial operation of photo-catalytic hydrogen evolution reactions (HER) in the availability of sacrificial reagents (SR).¹⁹⁷ In the research done by Jing *et al.*, CPCs contain the highest half incident beam angle of 14°, length of 0.4 m, and whole arm of 1.5 m, and pyrex reactor tubes 1.6 m in length were used. However, as particulate photo-catalytic reactor is scalable and it has low operation and maintenance cost, it is more effective than others.

Table 12: The benefits and drawbacks of different types of photo-reactors

Reactor	Findings	Drawbacks	Ref.
Slurry reactor	<ul style="list-style-type: none"> • Can be operated in fixed bed mode or continuous flow patterns • Combination of gas-liquid-solid phase 	<ul style="list-style-type: none"> • Continuous stirring causes the additional cost • Active contact surface for reaction is low 	28, 185
Fluidized reactor	<ul style="list-style-type: none"> • High photo-catalytic activity • Efficient rate of heat and matter transfer by vigorous excitation of solid 	<ul style="list-style-type: none"> • Abrasion of particles and attrition of the catalyst may causes erosion in reactor • difficult to separate from mixture 	188, 198
Optical reactor	<ul style="list-style-type: none"> • Surface area is larger • Efficiency of light utilization is higher • Efficient processing capacities of the catalyst 	<ul style="list-style-type: none"> • Deactivation catalyst at high temperature • Maximum reactor volume cannot be applying Uniform coating of fibers is complex 	188
Monolith reactor	<ul style="list-style-type: none"> • Ratio of surface to volume is higher • Pressure drop is low • Flow rate is higher 	<ul style="list-style-type: none"> • Light efficiency is low • Catalyst adhesion on wall is lower 	188,198,199
Fixed bed reactor	<ul style="list-style-type: none"> • large Surface area • minimum reaction period • lower Operating cost 	<ul style="list-style-type: none"> • low Light efficiency • lower adhesion 	188,198,199
Particulate photo-catalyst reactor	<ul style="list-style-type: none"> • Minimal fabrication cost • High scale up potential • Operating cost is lower 	<ul style="list-style-type: none"> • reactors tend to be bulky • water is required in large volumes 	186

Process Parameters for Photo Catalytic Reaction

- Light intensity or Irradiation of light
- Temperature effect
- PH effect
- Reactor design
- Oxygen vacancies
- Presence of Sacrificial agents
- Miscellaneous factors affect

Light Intensity

The higher hydrogen production rate is linearly related to light irradiation. The effectiveness of photo catalytic splitting of water can be improved with the rise in light intensity generating power more than the threshold level of activation.^{200, 201} Two regions are available related to the photo-catalytic reaction related to the UV photon flux. One region is for

laboratory research fluxes which are 25 mW cm⁻². Compare to the reaction of recombination the hole electron couple is consumed quicker in a chemical reaction. During the half-order region, the intensity remains higher, the recombination rate is a major factor and creates less change on the rate of the change the reaction process. The change of the value of the reaction rate is related to the wavelength which appears following the catalyst spectrum of the adsorption with a minimum reading level with respect to the band potential energy.²⁰² In the year 2013, Baniasadi *et al* announced that the rate of hydrogen generation from Zinc-Sulfide (ZnS), increased by 20% with rise in intensity range of light from 90 to 100 mW cm⁻².²⁰³ In another research work report by Leon and Tambago, indicated that the hydrogen (H₂) production increased using Cd_{0.4}Zn_{0.6}S while the intensity of light was increased.²⁰⁴

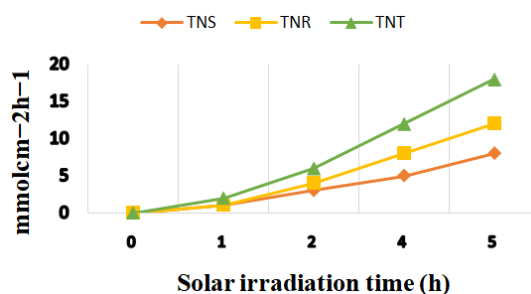


Fig .12: The comparison of photo-catalysts for hydrogen (H₂) generation under irradiation of solar Light for TNS (titanium nano sheet), TNT (titanium nano tube) and TNR (titanium nano rod).²⁰⁵

Table 13: Temperature effect on H₂ production rate

Sl. No.	Temperature °C	H ₂ production rate	Catalyst
01	30°C	59.00 mol/g.s	Pt/TiO ₂
02	40°C	92.00 mol/g.s	Pt/TiO ₂
03	50°C	370.00 mol/g.s	Pt/TiO ₂

Temperature Effect

The photo-catalytic behavior of catalyst material is introduced by temperature, since electron and hole generation is not related to it directly. But, the temperature has a crucial role to improve desorption of hydrogen gas (H₂) from the surface area of the considering catalyst to accelerate the effect of photo catalyst. It is thermodynamically established that, temperature ameliorates the reaction process in maximum cases. The rate of

change of applied temperature differs according to the change of catalyst. The photo-catalytic activity could be increased by the adjustment of the factor. The hydrogen (H₂) production becomes slower when the value of the temperature goes down. In this process desorption limits the reaction mechanism. The higher valance electron in the valance band will be transferred to higher energy levels during high-temperature conditions. The electron and hole generation will initiate oxidation & reduction reaction

respectively with charge carrier recombination.²⁰² In 30°C, 40°C, 50°C the hydrogen gas generation was 59, 92 & 370 mol/g.s respectively.²⁰⁶ Hydrogen generation increased from 4.71 mmol g⁻¹ to 15.18 mmol g⁻¹ after introducing a temperature rise from 45°C to 55°C.²⁰⁷ In a photocatalytic study it was found that the optimum temperature of this process should be 60°C to 80°C.²⁰⁸

pH Effect

The hydrogen (H₂) generation from water splitting depends on the concentration of the proton which indicates the pH of the regarding solution. In the water-splitting process, an electron is generated throughout the reaction process. A significant organic species is needed for the proton reforming. It is recommended to generate hydrogen in a strongly acidic solution rather than in a basic solution (pH>7). Similarly, the band gap potential shift also depends on pH value.²⁰ In a CuOx/TiO₂ catalytic medium with basic medium (pH 10) hydrogen production is maximum. The atom copper Cu (I) shows unstable behavior in TiO₂ based acidic medium. In the visible light TiO₂ part of the catalyst, Si/CdS/TiO₂/Pt is unstable in a strong base or acidic reaction.²⁰⁹ The optimum pH value of a photo-catalytic reaction for better hydrogen production rate in CuAlO₂/TiO₂ catalyst surface is 11.²¹⁰ The catalyst Pt/r-TiO₂ has the ability to produce hydrogen up to 56.6mmol in a pH condition at 5.5 during 4h of operation from pH value 12 to 2.0 (211).The hydrogen generation is 1200mmol g⁻¹ h⁻¹ in NiO/TiO₂ catalyst in a pH condition 6.6. So the hydrogen generation is directly depends on the according pH reading of the reaction where the best pH reading is about zero [0.00] charge value.²¹² In an acidic solution of methanol-water the photosensitized TiO₂/RuO₂-MV²⁺ catalyst can generate enough hydrogen (H₂).²¹³ The reduction reaction of hydrogen from H⁺ to H₂ can be increased when more protons are present on the surface of the regarding catalyst in an acidic solution (pH<7). The hydrogen generation is rapid in the acidic solution than in the basic solution.²⁰³ So in a photo-catalytic reaction the hydrogen production is better in the acidic solution.

Oxygen Vacancy

Oxygen vacancy is a significant factor to enhance H₂ production as well as the ionic longevity increase. Paucity of oxygen can be produced by applying

metal oxides with the process of catalyst synthesis, decreasing value and mixture.²¹⁴ When the titanium-oxide (TiO₂) is used as the titanium ion and oxygen gap are created at the same time. More titanium ions are produced because of the increasing oxygen gap. As a result, there is a situation of titanium defects, amorphous surface area disorder, and finally relative oxygen gap. This oxygen gap indirectly related to electron stability because of the absence of oxygen ion. Whereas, the regular lattice of the oxygen atom was taken by electrons, and the local state was formed by oxygen vacancies and Ti³⁺. Then, the VB holes of TiO₂ were generated and the electrons excited to the CB of TiO₂. At CB, the H⁺ reduce to H₂ through a reduction reaction.²¹⁵ So hydrogen gas generation without the recombination of the electron-hole and the amelioration of the charge longevity is the main aim to be achieved.

Reagent for Sacrificial Behavior

By introducing organic species in the reaction process the efficiency of the photo-catalyst can be improved. For example Methanol, Ethanol, phenol, and Glycerol can act as reaction agents which will be sacrificial. Relative to the water molecule, organic species behaves like a hole which will be a scavenger.²¹⁶ Photo-catalysis process is one of the major way of sustainable hydrogen production. Now the effect of the sacrificial agents in the way of hydrogen production must be fruitful. This hydrogen production can be accelerated using alcohol. This process is also known as photo-reforming. Because alcohol helps semiconductor in oxidation and reduction reaction. The activity order of sacrificial reagents is, Glycerol > Ethylene glycol > Methanol > Ethanol.²¹⁷ The hydrogen gas generation is a dependable factor with respect to the alpha hydrogen. Glycerol has a unique structure with five alpha hydrogen which is major than glycol, methanol and ethanol. On the other hand hydrogen generation is also have a relation with the concentration of alpha hydrogen and concentration of the agents.²¹⁸

Figure:-13 exhibits the outcome rate of hydrogen with the increment of methanol percentage and reaction time. It shows that at 5% methanol concentration the value hydrogen production rate is optimum. But further concentration rise does not help further in hydrogen production. The reason behind it may be the saturation of catalyst surface. When the surface

area of the photo-catalyst goes to a saturated level then the hydrogen production does not rise further.

So only a certain level of hydrogen production rate can be maintain from all the arrangement.

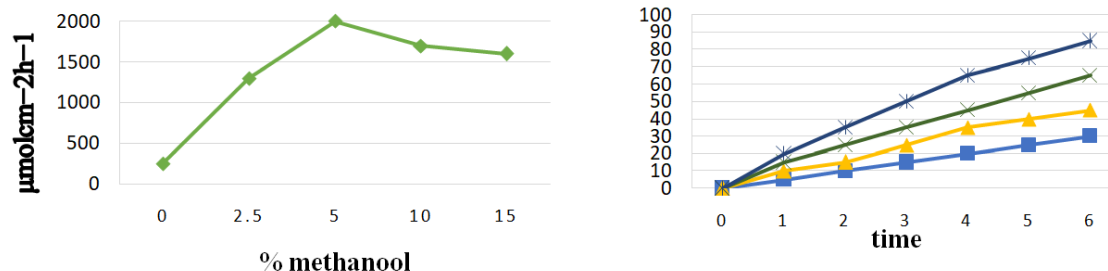


Fig.13 : The photo-catalysts comparison for hydrogen generation in the irradiation of solar Light for TNS, TNT and TNR²⁰⁵

Table 16:A Summary of numerous sacrificial reagents used in photo-catalytic H₂ production process

Year	Feed	Catalyst	Reactor/Parameter	Efficiency	Ref.
2019	10 % ethanol -water	.05 g TiO ₂ /MMT Quartz flask	Slurry reactor 40 W Xe lamp	methanol >ethylene glycol > ethanol >> propanol >Glycerol	219
2017	15% glycerol -water	85 mg 0.5 wt% Pt//TiO ₂	Pyrex reactor 130 W Hg lamp Medium pressure	Pt >Pd> Au glycerol > Propan-2-ol	220
2016	25 % n- propanol -water	50 mg 0.5 % RuO ₂ @TiO ₂	Glass reactor UV light Temperature at 25C	MeOH> t-BuOH > n- BuOH, PrOH> n-EtOH	221
2015	15% 2-propanol -water	0.065 g & 1 wt% Pd	Tubular reactor UV (375 nm, 10 mW cm-2)	Pd> Pt z Au. methanol > 2- ethanol >propanol >tert-butanol	222
2015	5% methanol -water	450 mL water solution,	Quartz reactor system 250 W Xe arc lamp, 30C under atmospheric pressure	ethylene > anhydrous glycol >Methanol	223
2015	5 % glycol -water	6.5 mg 1.5 wt% Au/P25	Tubular reactor SB-100P/F lamp (100 W, 265 nm)	Au/P25 > Au/brookite> Au/anatase	217

Conclusions

In comparison with cleanness and high calorific value Hydrogen is now a burning issue for today's energy regulatory authorities rather than other fuels like fossil, wind, solar, or another renewable. However, in nature H₂ is not available in free form (i.e. atomic state). Among various H₂ production process low-cost H₂ is available from fossil i.e. petrochemicals, but the main question that arises

here is the sustainability of this process. To ensure affordable and clean energy (SDG Goal-7) Sunlight to Hydrogen or STH is the best solution. While comparing with other traditional fuels H₂ is a Future dominating fuel with its best transportation, storage, transmission, and cleanness. Photo catalysis is the best way to achieve maximum STH conversion with less set-up and reagent cost. However, there are still so many technical drawbacks in catalytic

water splitting as this technique still not mature enough. Several researchers are trying to develop this process from the different technical corners like catalyst development, process parameter optimization, reactor design, etc. Some other catalyst development techniques like Sensitization with noble metal loading, Increasing Photo catalytically Active Area, modification of Surface with graphene and other Carbonaceous material, Formation of Solid Solutions, and Modification of Photo-catalysts with Co-catalysts are also studied to develop Photocatalytic efficiency of catalysts. Among all techniques doping, Heterojunction and Dye sensitization shed a light on development techniques for efficient catalyst synthesis. Within this three-technique, the development of doping in the different catalysts is the most promising one. Doping in the catalyst surface may extend its photonic response from the UV region to the visible length of electromagnetic radiation by forming an impure energy band. However, there is still a lot to work on the photocatalytic water splitting process for better understanding and smooth future of this process.

Highlights

- Photo-catalytic water splitting is a promising Green-Harvesting technique among all H₂ generation methods
- Doping, Heterojunction and Dye sensitization shed a light on development strategies
- Elemental doping exhibit's maximum efficiency while doping with rare earth metals

Acknowledgements

The authors would like to acknowledge Bangladesh Council of Scientific and Industrial Research (BCSIR) & Hydrogen Energy Laboratory project for its Scholastic and technical support.

Funding

This research did not receive any specific grant from funding agencies in the public or commercial sectors.

Conflict of Interest

The author(s) declared no potential competing interest with respect to the research, authorship, and/or publication of this article.

References

1. Shafiee S, Topal E. When will fossil fuel reserves be diminished? *Energy policy*. 2009;37(1):181-9.
2. Höök M, Tang X. Depletion of fossil fuels and anthropogenic climate change—A review. *Energy policy*. 2013;52:797-809.
3. Bhandari R, Trudewind CA, Zapp P. Life cycle assessment of hydrogen production via electrolysis—a review. *Journal of cleaner production*. 2014;85:151-63.
4. Kumaravel V, Mathew S, Bartlett J, Pillai SC. Photocatalytic hydrogen production using metal doped TiO₂: A review of recent advances. *Applied Catalysis B: Environmental*. 2019;244:1021-64.
5. Balta MT, Dincer I, Hepbasli A. Thermodynamic assessment of geothermal energy use in hydrogen production. *International Journal of hydrogen energy*. 2009;34(7):2925-39.
6. Dincer I, Acar C. Review and evaluation of hydrogen production methods for better sustainability. *International journal of hydrogen energy*. 2015;40(34):11094-111.
7. Dincer I. Green methods for hydrogen production. *International journal of hydrogen energy*. 2012;37(2):1954-71.
8. Acar C, Dincer I, Naterer GF. Review of photocatalytic water-splitting methods for sustainable hydrogen production. *International Journal of Energy Research*. 2016;40(11):1449-73.
9. Kotay SM, Das D. Biohydrogen as a renewable energy resource—prospects and potentials. *International Journal of Hydrogen Energy*. 2008;33(1):258-63.
10. Koutrouli EC, Kalfas H, Gavala HN, Skiadas IV, Stamatelatou K, Lyberatos G. Hydrogen and methane production through two-stage mesophilic anaerobic digestion of olive pulp. *Bioresource technology*. 2009;100(15):3718-23.
11. Das D, Veziroglu TN. Advances in biological hydrogen production processes. *International journal of hydrogen energy*. 2008;33(21):6046-57.
12. Lodhi M. Hydrogen production from renewable sources of energy. *International journal of hydrogen energy*. 1987;12(7):461-8.

13. Guo L, Chen Y, Su J, Liu M, Liu Y. Obstacles of solar-powered photocatalytic water splitting for hydrogen production: A perspective from energy flow and mass flow. *Energy*. 2019;172:1079-86.
14. Fujishima A, Honda K. Electrochemical photolysis of water at a semiconductor electrode. *nature*. 1972;238(5358):37-8.
15. Zou Z, Ye J, Sayama K, Arakawa H. Direct splitting of water under visible light irradiation with an oxide semiconductor photocatalyst. *Materials For Sustainable Energy: A Collection of Peer-Reviewed Research and Review Articles from Nature Publishing Group: World Scientific*; 2011. p. 293-5.
16. Wang H, Zhang L, Chen Z, Hu J, Li S, Wang Z, *et al.* Semiconductor heterojunction photocatalysts: design, construction, and photocatalytic performances. *Chemical Society Reviews*. 2014;43(15):5234-44.
17. Chen X, Shen S, Guo L, Mao SS. Semiconductor-based photocatalytic hydrogen generation. *Chemical reviews*. 2010;110(11):6503-70.
18. An X, Hu C, Liu H, Qu J. Hierarchical nanotubular anatase/rutile/TiO₂ (B) heterophase junction with oxygen vacancies for enhanced photocatalytic H₂ production. *Langmuir*. 2018;34(5):1883-9.
19. Zhang C, Zhou Y, Bao J, Zhang Y, Fang J, Zhao S, *et al.* Sn²⁺-Doped Double-Shelled TiO₂ Hollow Nanospheres with Minimal Pt Content for Significantly Enhanced Solar H₂ Production. *ACS Sustainable Chemistry & Engineering*. 2018;6(5):7128-37.
20. Hainer AS, Hodgins JS, Sandre V, Vallieres M, Lanterna AE, Scaiano JC. Photocatalytic hydrogen generation using metal-decorated TiO₂: sacrificial donors vs true water splitting. *ACS Energy Letters*. 2018;3(3):542-5.
21. Xu Q, Cheng B, Yu J, Liu G. Making co-condensed amorphous carbon/g-C₃N₄ composites with improved visible-light photocatalytic H₂-production performance using Pt as cocatalyst. *Carbon*. 2017;118:241-9.
22. Jo W-K, Selvam NCS. Z-scheme CdS/g-C₃N₄ composites with RGO as an electron mediator for efficient photocatalytic H₂ production and pollutant degradation. *Chemical Engineering Journal*. 2017;317:913-24.
23. Liu X, Wang P, Zhai H, Zhang Q, Huang B, Wang Z, *et al.* Synthesis of synergetic phosphorus and cyano groups (CN) modified g-C₃N₄ for enhanced photocatalytic H₂ production and CO₂ reduction under visible light irradiation. *Applied Catalysis B: Environmental*. 2018;232:521-30.
24. Vaquero F, Navarro R, Fierro J. Influence of the solvent on the structure, morphology and performance for H₂ evolution of CdS photocatalysts prepared by solvothermal method. *Applied Catalysis B: Environmental*. 2017;203:753-67.
25. Zhang M, Lin H, Cao J, Guo X, Chen S. Construction of novel S/CdS type II heterojunction for photocatalytic H₂ production under visible light: the intrinsic positive role of elementary α-S. *Chemical Engineering Journal*. 2017;321:484-94.
26. Qin N, Xiong J, Liang R, Liu Y, Zhang S, Li Y, *et al.* Highly efficient photocatalytic H₂ evolution over MoS₂/CdS-TiO₂ nanofibers prepared by an electrospinning mediated photodeposition method. *Applied Catalysis B: Environmental*. 2017;202:374-80.
27. Dincer I, Acar C. A review on clean energy solutions for better sustainability. *International Journal of Energy Research*. 2015;39(5):585-606.
28. Fajrina N, Tahir M. A critical review in strategies to improve photocatalytic water splitting towards hydrogen production. *International Journal of Hydrogen Energy*. 2019;44(2):540-77.
29. Haselmann GM, Eder D. Early-stage deactivation of platinum-loaded TiO₂ using in situ photodeposition during photocatalytic hydrogen evolution. *ACS Catalysis*. 2017;7(7):4668-75.
30. Tiwari A, Krishna NV, Giribabu L, Pal U. Hierarchical porous TiO₂ embedded unsymmetrical zinc-Phthalocyanine sensitizer for visible-light-Induced photocatalytic H₂ production. *The Journal of Physical Chemistry C*. 2018;122(1):495-502.
31. Guayaquil-Sosa JF. Photocatalytic Hydrogen Production using a Mesoporous TiO₂ Doped with Pt: Semiconductor Synthesis, Oxidation-Reduction Network and Quantum Efficiencies. 2018.

32. Hou H-J, Zhang X-H, Huang D-K, Ding X, Wang S-Y, Yang X-L, *et al.* Conjugated microporous poly (benzothiadiazole)/TiO₂ heterojunction for visible-light-driven H₂ production and pollutant removal. *Applied Catalysis B: Environmental*. 2017;203:563-71.
33. Seadira TW, Sadanandam G, Ntho T, Masuku CM, Scurrrell MS. Preparation and characterization of metals supported on nanostructured TiO₂ hollow spheres for production of hydrogen via photocatalytic reforming of glycerol. *Applied Catalysis B: Environmental*. 2018;222:133-45.
34. Murakami N, Chiyoya T, Tsubota T, Ohno T. Switching redox site of photocatalytic reaction on titanium (IV) oxide particles modified with transition-metal ion controlled by irradiation wavelength. *Applied Catalysis A: General*. 2008;348(1):148-52.
35. Gholipour MR, Dinh C-T, Béland F, Do T-O. Nanocomposite heterojunctions as sunlight-driven photocatalysts for hydrogen production from water splitting. *Nanoscale*. 2015;7(18):8187-208.
36. Avilés-García O, Espino-Valencia J, Romero R, Rico-Cerda JL, Arroyo-Albiter M, Natividad R. W and Mo doped TiO₂: synthesis, characterization and photocatalytic activity. *Fuel*. 2017;198:31-41.
37. Hussain M, Ceccarelli R, Marchisio D, Fino D, Russo N, Geobaldo F. Synthesis, characterization, and photocatalytic application of novel TiO₂ nanoparticles. *Chemical Engineering Journal*. 2010;157(1):45-51.
38. Zhang G, Lin L, Li G, Zhang Y, Savateev A, Zafeiratos S, *et al.* Ionothermal Synthesis of Triazine–Heptazine-Based Copolymers with Apparent Quantum Yields of 60% at 420 nm for Solar Hydrogen Production from “Sea Water”. *Angewandte Chemie International Edition*. 2018;57(30):9372-6.
39. Sudha D, Sivakumar P. Review on the photocatalytic activity of various composite catalysts. *Chemical Engineering and Processing: Process Intensification*. 2015;97:112-33.
40. Bashiri R, Mohamed NM, Kait CF, Sufian S. Hydrogen production from water photosplitting using Cu/TiO₂ nanoparticles: Effect of hydrolysis rate and reaction medium. *International Journal of Hydrogen Energy*. 2015;40(18):6021-37.
41. Huang H, Dai B, Wang W, Lu C, Kou J, Ni Y, *et al.* Oriented built-in electric field introduced by surface gradient diffusion doping for enhanced photocatalytic H₂ evolution in CdS nanorods. *Nano Letters*. 2017;17(6):3803-8.
42. Shi R, Ye HF, Liang F, Wang Z, Li K, Weng Y, *et al.* Interstitial P-Doped CdS with Long-Lived Photogenerated Electrons for Photocatalytic Water Splitting without Sacrificial Agents. *Advanced Materials*. 2018;30(6):1705941.
43. Zhang L, Liu D, Guan J, Chen X, Guo X, Zhao F, *et al.* Metal-free g-C₃N₄ photocatalyst by sulfuric acid activation for selective aerobic oxidation of benzyl alcohol under visible light. *Materials Research Bulletin*. 2014;59:84-92.
44. Deng F, Zou J-P, Zhao L-N, Zhou G, Luo X-B, Luo S-L. Nanomaterial-Based Photocatalytic Hydrogen Production. *Nanomaterials for the Removal of Pollutants and Resource Reutilization: Elsevier*; 2019. p. 59-82.
45. Chen M, Liu Y, Li C, Li A, Chang X, Liu W, *et al.* Spatial control of cocatalysts and elimination of interfacial defects towards efficient and robust CIGS photocathodes for solar water splitting. *Energy & Environmental Science*. 2018;11(8):2025-34.
46. Munoz-Batista MJ, Fontelles-Carceller O, Ferrer M, Fernández-García M, Kubacka A. Disinfection capability of Ag/g-C₃N₄ composite photocatalysts under UV and visible light illumination. *Applied Catalysis B: Environmental*. 2016;183:86-95.
47. Singh R, Dutta S. A review on H₂ production through photocatalytic reactions using TiO₂/TiO₂-assisted catalysts. *Fuel*. 2018;220:607-20.
48. Chiu I, Lin S-X, Kao C-T, Wu R-J. Promoting hydrogen production by loading PdO and Pt on N-TiO₂ under visible light. *International journal of hydrogen energy*. 2014;39(27):14574-80.
49. Lai C-L, Huang H-L, Shen J-H, Wang K-K, Gan D. The formation of anatase TiO₂ from TiO nanocrystals in sol-gel process. *Ceramics International*. 2015;41(3):5041-8.
50. Sun T, Liu E, Fan J, Hu X, Wu F, Hou W, *et al.* High photocatalytic activity of hydrogen production from water over Fe doped and Ag deposited anatase TiO₂

- catalyst synthesized by solvothermal method. *Chemical engineering journal*. 2013;228:896-906.
51. Tian M, Wang H, Sun D, Peng W, Tao W. Visible light driven nanocrystal anatase TiO₂ doped by Ce from sol-gel method and its photoelectrochemical water splitting properties. *International journal of hydrogen energy*. 2014;39(25):13448-53.
 52. Gao H, Zhang P, Zhao J, Zhang Y, Hu J, Shao G. Plasmon enhancement on photocatalytic hydrogen production over the Z-scheme photosynthetic heterojunction system. *Applied Catalysis B: Environmental*. 2017;210:297-305.
 53. Fan X, Fan J, Hu X, Liu E, Kang L, Tang C, *et al.* Preparation and characterization of Ag deposited and Fe doped TiO₂ nanotube arrays for photocatalytic hydrogen production by water splitting. *Ceramics International*. 2014;40(10):15907-17.
 54. Fornari AMD, de Araujo MB, Duarte CB, Machado G, Teixeira SR, Weibel DE. Photocatalytic reforming of aqueous formaldehyde with hydrogen generation over TiO₂ nanotubes loaded with Pt or Au nanoparticles. *International Journal of Hydrogen Energy*. 2016;41(27):11599-607.
 55. Xing Z, Zong X, Butburee T, Pan J, Bai Y, Wang L. Nanohybrid materials of titania nanosheets and plasmonic gold nanoparticles for effective hydrogen evolution. *Applied Catalysis A: General*. 2016;521:96-103.
 56. Zou Y, Kang S-Z, Li X, Qin L, Mu J. TiO₂ nanosheets loaded with Cu: A low-cost efficient photocatalytic system for hydrogen evolution from water. *International journal of hydrogen energy*. 2014;39(28):15403-10.
 57. Badawy MI, Ali ME, Ghaly MY, El-Missiry MA. Mesoporous simonkolleite-TiO₂ nanostructured composite for simultaneous photocatalytic hydrogen production and dye decontamination. *Process Safety and Environmental Protection*. 2015;94:11-7.
 58. Tian H, Kang S-Z, Li X, Qin L, Ji M, Mu J. Fabrication of an efficient noble metal-free TiO₂-based photocatalytic system using Cu-Ni bimetallic deposit as an active center of H₂ evolution from water. *Solar Energy Materials and Solar Cells*. 2015;134:309-17.
 59. Yan Z, Yu X, Han A, Xu P, Du P. Noble-metal-free Ni (OH) 2-modified CdS/reduced graphene oxide nanocomposite with enhanced photocatalytic activity for hydrogen production under visible light irradiation. *The Journal of Physical Chemistry C*. 2014;118(40):22896-903.
 60. Chiarello GL, Dozzi MV, Scavini M, Grunwaldt J-D, Selli E. One step flame-made fluorinated Pt/TiO₂ photocatalysts for hydrogen production. *Applied Catalysis B: Environmental*. 2014;160:144-51.
 61. Ong W-J, Tan L-L, Ng YH, Yong S-T, Chai S-P. Graphitic carbon nitride (g-C₃N₄)-based photocatalysts for artificial photosynthesis and environmental remediation: are we a step closer to achieving sustainability? *Chemical reviews*. 2016;116(12):7159-329.
 62. Kang HW, Park SB, Kim JG, Kim IT. Effects of F for enhancement of H₂ evolution on visible-light-driven photocatalyst of SrTiO₃: Cr/Ta/F prepared by spray pyrolysis. *International journal of hydrogen energy*. 2014;39(11):5537-45.
 63. Shen P, Lofaro Jr JC, Woerner WR, White MG, Su D, Orlov A. Photocatalytic activity of hydrogen evolution over Rh doped SrTiO₃ prepared by polymerizable complex method. *Chemical engineering journal*. 2013;223:200-8.
 64. Zhang H, Chen G, Li Y, Teng Y. Electronic structure and photocatalytic properties of copper-doped CaTiO₃. *International journal of hydrogen energy*. 2010;35(7):2713-6.
 65. Sun X, Xie Y, Wu F, Chen H, Lv M, Ni S, *et al.* Photocatalytic hydrogen production over chromium doped layered perovskite Sr₂TiO₄. *Inorganic chemistry*. 2015;54(15):7445-53.
 66. Zou J-P, Zhang L-Z, Luo S-L, Leng L-H, Luo X-B, Zhang M-J, *et al.* Preparation and photocatalytic activities of two new Zn-doped SrTiO₃ and BaTiO₃ photocatalysts for hydrogen production from water without cocatalysts loading. *International journal of hydrogen energy*. 2012;37(22):17068-77.
 67. Yu H, Wang J, Yan S, Yu T, Zou Z. Elements doping to expand the light response of SrTiO₃. *Journal of Photochemistry and Photobiology A: Chemistry*. 2014;275:65-71.
 68. Kang HW, Park SB. H₂ evolution under visible light irradiation from aqueous methanol solution on SrTiO₃: Cr/Ta prepared by

- spray pyrolysis from polymeric precursor. *International journal of hydrogen energy*. 2011;36(16):9496-504.
69. Lu L, Ni S, Liu G, Xu X. Structural dependence of photocatalytic hydrogen production over La/Cr co-doped perovskite compound ATiO_3 (A= Ca, Sr and Ba). *International Journal of Hydrogen Energy*. 2017;42(37):23539-47.
70. Zhang H, Chen G, He X, Xu J. Electronic structure and photocatalytic properties of Ag–La codoped CaTiO_3 . *Journal of alloys and compounds*. 2012;516:91-5.
71. Kang HW, Park SB. Improved performance of tri-doped photocatalyst SrTiO_3 : Rh/Ta/F for H_2 evolution under visible light irradiation. *International Journal of Hydrogen Energy*. 2016;41(32):13970-8.
72. Cao S, Low J, Yu J, Jaroniec M. Polymeric photocatalysts based on graphitic carbon nitride. *Advanced Materials*. 2015;27(13):2150-76.
73. Liu J, Zhang T, Wang Z, Dawson G, Chen W. Simple pyrolysis of urea into graphitic carbon nitride with recyclable adsorption and photocatalytic activity. *Journal of Materials Chemistry*. 2011;21(38):14398-401.
74. Pang X, Bian H, Wang W, Liu C, Khan MS, Wang Q, *et al.* A bio-chemical application of N-GQDs and g- C_3N_4 QDs sensitized TiO_2 nanopillars for the quantitative detection of pcDNA3-HBV. *Biosensors and Bioelectronics*. 2017;91:456-64.
75. Patnaik S, Martha S, Parida K. An overview of the structural, textural and morphological modulations of g- C_3N_4 towards photocatalytic hydrogen production. *Rsc Advances*. 2016;6(52):46929-51.
76. Li C, Luo Z, Wang T, Gong J. Surface, Bulk, and Interface: Rational Design of Hematite Architecture toward Efficient Photo-Electrochemical Water Splitting. *Advanced Materials*. 2018;30(30):1707502.
77. Zhong Y, Wang Z, Feng J, Yan S, Zhang H, Li Z, *et al.* Improvement in photocatalytic H_2 evolution over g- C_3N_4 prepared from protonated melamine. *Applied surface science*. 2014;295:253-9.
78. Ma L, Fan H, Li M, Tian H, Fang J, Dong G. A simple melamine-assisted exfoliation of polymeric graphitic carbon nitrides for highly efficient hydrogen production from water under visible light. *Journal of Materials Chemistry A*. 2015;3(44):22404-12.
79. Wang Y, Zhao S, Zhang Y, Fang J, Zhou Y, Yuan S, *et al.* One-pot synthesis of K-doped g- C_3N_4 nanosheets with enhanced photocatalytic hydrogen production under visible-light irradiation. *Applied Surface Science*. 2018;440:258-65.
80. Liu M, Xia P, Zhang L, Cheng B, Yu J. Enhanced photocatalytic H_2 -production activity of g- C_3N_4 nanosheets via optimal photodeposition of Pt as cocatalyst. *ACS Sustainable Chemistry & Engineering*. 2018;6(8):10472-80.
81. Maeda K, Domen K. Photocatalytic water splitting: recent progress and future challenges. *The Journal of Physical Chemistry Letters*. 2010;1(18):2655-61.
82. Humayun M, Fu Q, Zheng Z, Li H, Luo W. Improved visible-light catalytic activities of novel Au/P-doped g- C_3N_4 photocatalyst for solar fuel production and mechanism. *Applied Catalysis A: General*. 2018;568:139-47.
83. Yan X, Jia Z, Che H, Chen S, Hu P, Wang J, *et al.* A selective ion replacement strategy for the synthesis of copper doped carbon nitride nanotubes with improved photocatalytic hydrogen evolution. *Applied Catalysis B: Environmental*. 2018;234:19-25.
84. Sun C, Zhang H, Liu H, Zheng X, Zou W, Dong L, *et al.* Enhanced activity of visible-light photocatalytic H_2 evolution of sulfur-doped g- C_3N_4 photocatalyst via nanoparticle metal Ni as cocatalyst. *Applied Catalysis B: Environmental*. 2018;235:66-74.
85. Qi K, Xie Y, Wang R, Liu S-y, Zhao Z. Electroless plating Ni-P cocatalyst decorated g- C_3N_4 with enhanced photocatalytic water splitting for H_2 generation. *Applied Surface Science*. 2019;466:847-53.
86. Chen P-W, Li K, Yu Y-X, Zhang W-D. Cobalt-doped graphitic carbon nitride photocatalysts with high activity for hydrogen evolution. *Applied Surface Science*. 2017;392:608-15.
87. Jo W-K, Kumar S, Eslava S, Tonda S. Construction of $\text{Bi}_2\text{WO}_6/\text{RGO}/\text{g-C}_3\text{N}_4$ 2D/2D/2D hybrid Z-scheme heterojunctions with large interfacial contact area for efficient charge separation and high-performance photoreduction of CO_2 and H_2O into solar fuels. *Applied Catalysis B: Environmental*.

- 2018;239:586-98.
88. Huang Z, Li F, Chen B, Yuan G. Porous and low-defected graphitic carbon nitride nanotubes for efficient hydrogen evolution under visible light irradiation. *RSC Advances*. 2015;5(124):102700-6.
89. Zhou Y, Zhang L, Huang W, Kong Q, Fan X, Wang M, *et al.* N-doped graphitic carbon-incorporated g-C₃N₄ for remarkably enhanced photocatalytic H₂ evolution under visible light. *Carbon*. 2016;99:111-7.
90. Chen J, Hong Z, Chen Y, Lin B, Gao B. One-step synthesis of sulfur-doped and nitrogen-deficient g-C₃N₄ photocatalyst for enhanced hydrogen evolution under visible light. *Materials Letters*. 2015;145:129-32.
91. Lan Z-A, Zhang G, Wang X. A facile synthesis of Br-modified g-C₃N₄ semiconductors for photoredox water splitting. *Applied Catalysis B: Environmental*. 2016;192:116-25.
92. Wang H, Bian Y, Hu J, Dai L. Highly crystalline sulfur-doped carbon nitride as photocatalyst for efficient visible-light hydrogen generation. *Applied Catalysis B: Environmental*. 2018;238:592-8.
93. Wu M, Zhang J, He B-b, Wang H-w, Wang R, Gong Y-s. In-situ construction of coral-like porous P-doped g-C₃N₄ tubes with hybrid 1D/2D architecture and high efficient photocatalytic hydrogen evolution. *Applied Catalysis B: Environmental*. 2019;241:159-66.
94. Zhang J-W, Gong S, Mahmood N, Pan L, Zhang X, Zou J-J. Oxygen-doped nanoporous carbon nitride via water-based homogeneous supramolecular assembly for photocatalytic hydrogen evolution. *Applied Catalysis B: Environmental*. 2018;221:9-16.
95. Wang H, Yang C, Li M, Chen F, Cui Y. Enhanced photocatalytic hydrogen production of restructured B/F codoped g-C₃N₄ via post-thermal treatment. *Materials Letters*. 2018;212:319-22.
96. Guo S, Tang Y, Xie Y, Tian C, Feng Q, Zhou W, *et al.* P-doped tubular g-C₃N₄ with surface carbon defects: universal synthesis and enhanced visible-light photocatalytic hydrogen production. *Applied Catalysis B: Environmental*. 2017;218:664-71.
97. Zhang J, Huang F. Enhanced visible light photocatalytic H₂ production activity of g-C₃N₄ via carbon fiber. *Applied Surface Science*. 2015;358:287-95.
98. Wu Z, Gao H, Yan S, Zou Z. Synthesis of carbon black/carbon nitride intercalation compound composite for efficient hydrogen production. *Dalton Transactions*. 2014;43(31):12013-7.
99. Li Z, Luo W, Zhang M, Feng J, Zou Z. Photoelectrochemical cells for solar hydrogen production: current state of promising photoelectrodes, methods to improve their properties, and outlook. *Energy & Environmental Science*. 2013;6(2):347-70.
100. Park Y, McDonald KJ, Choi K-S. Progress in bismuth vanadate photoanodes for use in solar water oxidation. *Chemical Society Reviews*. 2013;42(6):2321-37.
101. Jo WJ, Jang JW, Kong KJ, Kang HJ, Kim JY, Jun H, *et al.* Phosphate doping into monoclinic BiVO₄ for enhanced photoelectrochemical water oxidation activity. *Angewandte Chemie International Edition*. 2012;51(13):3147-51.
102. Jia Q, Iwashina K, Kudo A. Facile fabrication of an efficient BiVO₄ thin film electrode for water splitting under visible light irradiation. *Proceedings of the National Academy of Sciences*. 2012;109(29):11564-9.
103. Choi SK, Choi W, Park H. Solar water oxidation using nickel-borate coupled BiVO₄ photoelectrodes. *Physical Chemistry Chemical Physics*. 2013;15(17):6499-507.
104. Lianos P. Review of recent trends in photoelectrocatalytic conversion of solar energy to electricity and hydrogen. *Applied Catalysis B: Environmental*. 2017;210:235-54.
105. Fang L, Nan F, Yang Y, Cao D. Enhanced photoelectrochemical and photocatalytic activity in visible-light-driven Ag/BiVO₄ inverse opals. *Applied Physics Letters*. 2016;108(9):093902.
106. Zhong DK, Choi S, Gamelin DR. Near-complete suppression of surface recombination in solar photoelectrolysis by "Co-Pi" catalyst-modified W: BiVO₄. *Journal of the American Chemical Society*. 2011;133(45):18370-7.
107. Surendranath Y, Kanan MW, Nocera DG. Mechanistic studies of the oxygen evolution reaction by a cobalt-phosphate catalyst at neutral pH. *Journal of the American Chemical Society*. 2010;132(46):16501-9.
108. Rohloff M, Anke B, Zhang S, Gernert U,

- Scheu C, Lerch M, *et al.* Mo-doped BiVO₄ thin films—high photoelectrochemical water splitting performance achieved by a tailored structure and morphology. *Sustainable Energy & Fuels*. 2017;1(8):1830-46.
109. Soltani T, Tayyebi A, Lee B-K. Efficient promotion of charge separation with reduced graphene oxide (rGO) in BiVO₄/rGO photoanode for greatly enhanced photoelectrochemical water splitting. *Solar Energy Materials and Solar Cells*. 2018;185:325-32.
110. Wang T, Li C, Ji J, Wei Y, Zhang P, Wang S, *et al.* Reduced graphene oxide (rGO)/BiVO₄ composites with maximized interfacial coupling for visible light photocatalysis. *ACS Sustainable Chemistry & Engineering*. 2014;2(10):2253-8.
111. Rohloff M, Anke Br, Kasian O, Zhang S, Lerch M, Scheu C, *et al.* Enhanced Photoelectrochemical Water Oxidation Performance by Fluorine Incorporation in BiVO₄ and Mo: BiVO₄ Thin Film Photoanodes. *ACS applied materials & interfaces*. 2019;11(18):16430-42.
112. Kiani F, Astani NA, Rahighi R, Tayyebi A, Tayebi M, Khezri J, *et al.* Effect of graphene oxide nanosheets on visible light-assisted antibacterial activity of vertically-aligned copper oxide nanowire arrays. *Journal of colloid and interface science*. 2018;521:119-31.
113. Luo W, Yang Z, Li Z, Zhang J, Liu J, Zhao Z, *et al.* Solar hydrogen generation from seawater with a modified BiVO₄ photoanode. *Energy & Environmental Science*. 2011;4(10):4046-51.
114. Yang Y, Kang L, Li H. Enhancement of photocatalytic hydrogen production of BiFeO₃ by Gd³⁺ doping. *Ceramics International*. 2019;45(6):8017-22.
115. Fujishima A, Honda K. Electrochemical evidence for the mechanism of the primary stage of photosynthesis. *Bulletin of the chemical society of Japan*. 1971;44(4):1148-50.
116. Liu H, Xu C, Li D, Jiang HL. Photocatalytic hydrogen production coupled with selective benzylamine oxidation over MOF composites. *Angewandte Chemie International Edition*. 2018;57(19):5379-83.
117. Goto Y, Hisatomi T, Wang Q, Higashi T, Ishikiriya K, Maeda T, *et al.* A particulate photocatalyst water-splitting panel for large-scale solar hydrogen generation. *Joule*. 2018;2(3):509-20.
118. Lyu H, Hisatomi T, Goto Y, Yoshida M, Higashi T, Katayama M, *et al.* An Al-doped SrTiO₃ photocatalyst maintaining sunlight-driven overall water splitting activity for over 1000 h of constant illumination. *Chemical science*. 2019;10(11):3196-201.
119. Ohtani B. Preparing articles on photocatalysis—beyond the illusions, misconceptions, and speculation. *Chemistry letters*. 2008;37(3):216-29.
120. Jeong H, Kim T, Kim D, Kim K. Hydrogen production by the photocatalytic overall water splitting on NiO/Sr₃Ti₂O₇: effect of preparation method. *International journal of hydrogen energy*. 2006;31(9):1142-6.
121. Nishimoto S, Matsuda M, Miyake M. Photocatalytic activities of Rh-doped CaTiO₃ under visible light irradiation. *Chemistry letters*. 2006;35(3):308-9.
122. Ko Y-G, Lee WY. Effects of nickel-loading method on the water-splitting activity of a layered NiO x/Sr₄Ti₃O₁₀ photocatalyst. *Catalysis letters*. 2002;83(3-4):157-60.
123. Moon S-C, Mametsuka H, Suzuki E, Anpo M. Stoichiometric decomposition of pure water over Pt-loaded Ti/B binary oxide under UV-irradiation. *Chemistry letters*. 1998;27(2):117-8.
124. Ikeda S, Hara M, Kondo JN, Domen K, Takahashi H, Okubo T, *et al.* Preparation of a high active photocatalyst, K₂La₂Ti₃O₁₀, by polymerized complex method and its photocatalytic activity of water splitting. *Journal of materials research*. 1998;13(4):852-5.
125. Sayama K, Arakawa H. Effect of carbonate salt addition on the photocatalytic decomposition of liquid water over Pt-TiO₂ catalyst. *Journal of the Chemical Society, Faraday Transactions*. 1997;93(8):1647-54.
126. Tabata S, Nishida H, Masaki Y, Tabata K. Stoichiometric photocatalytic decomposition of pure water in Pt/TiO₂ aqueous suspension system. *Catalysis letters*. 1995;34(1-2):245-9.
127. Kudo A, Sayama K, Tanaka A, Asakura K, Domen K, Maruya K, *et al.* Nickel-loaded K₄Nb₆O₁₇ photocatalyst in the decomposition

- of H₂O into H₂ and O₂: Structure and reaction mechanism. *Journal of catalysis*. 1989;120(2):337-52.
128. Yamaguti K, Sato S. Photolysis of water over metallized powdered titanium dioxide. *Journal of the Chemical Society, Faraday Transactions 1: Physical Chemistry in Condensed Phases*. 1985;81(5):1237-46.
129. Lehn J. Photochemical water splitting continuous generation of hydrogen and oxygen by irradiation of aqueous suspensions of metal loaded strontium titanate. 1980.
130. Domen K, Naito S, Soma M, Onishi T, Tamaru K. Photocatalytic decomposition of water vapour on an NiO–SrTiO₃ catalyst. *Journal of the Chemical Society, Chemical Communications*. 1980(12):543-4.
131. Domen K, Naito S, Onishi T, Tamaru K, Soma M. Study of the photocatalytic decomposition of water vapor over a nickel (II) oxide-strontium titanate (SrTiO₃) catalyst. *The Journal of Physical Chemistry*. 1982;86(18):3657-61.
132. Lee WC, Tan L-L, Sumathi S, Chai S-P. Copper-doped flower-like molybdenum disulfide/bismuth sulfide photocatalysts for enhanced solar water splitting. *International Journal of Hydrogen Energy*. 2018;43(2):748-56.
133. Wang SY, Ko TS, Huang CC, Huang YS. Optical and electrical properties of MoS₂ and Fe-doped MoS₂. *Japanese Journal of Applied Physics*. 2014;53(4S):04EH7.
134. Lee WC, Gui M-M, Tan L-L, Wu TY, Sumathi S, Chai S-P. Bismuth sulphide-modified molybdenum disulphide as an efficient photocatalyst for hydrogen production under simulated solar light. *Catalysis Communications*. 2017;98:66-70.
135. Li H, Tu W, Zhou Y, Zou Z. Z-Scheme photocatalytic systems for promoting photocatalytic performance: recent progress and future challenges. *Advanced Science*. 2016;3(11):1500389.
136. Yamaguti K, Sato S. Water photolysis over metallized SrTiO₃ catalysts. *Nouveau journal de chimie* (1977). 1986;10(4-5):217-21.
137. Domen K, Kudo A, Onishi T. Mechanism of photocatalytic decomposition of water into H₂ and O₂ over NiO·SrTiO₃. *Journal of Catalysis*. 1986;102(1):92-8.
138. Domen K, Kudo A, Onishi T, Kosugi N, Kuroda H. Photocatalytic decomposition of water into hydrogen and oxygen over nickel (II) oxide-strontium titanate (SrTiO₃) powder. 1. Structure of the catalysts. *The Journal of Physical Chemistry*. 1986;90(2):292-5.
139. Miseki Y, Kato H, Kudo A. Water splitting into H₂ and O₂ over Cs₂Nb₄O₁₁ photocatalyst. *Chemistry letters*. 2005;34(1):54-5.
140. Ebina Y, Sakai N, Sasaki T. Photocatalyst of lamellar aggregates of RuO x-loaded perovskite nanosheets for overall water splitting. *The Journal of Physical Chemistry B*. 2005;109(36):17212-6.
141. Kudo A, Tanaka A, Domen K, Onishi T. The effects of the calcination temperature of SrTiO₃ powder on photocatalytic activities. *Journal of Catalysis*. 1988;111(2):296-301.
142. Abe R, Higashi M, Sayama K, Abe Y, Sugihara H. Photocatalytic activity of R₃MO₇ and R₂Ti₂O₇ (R= Y, Gd, La; M= Nb, Ta) for water splitting into H₂ and O₂. *The Journal of Physical Chemistry B*. 2006;110(5):2219-26.
143. Abe R, Higashi M, Zou Z, Sayama K, Abe Y. Photocatalytic water splitting into H₂ and O₂ over R₂Ti₂O₇ (R= Y, rare earth) with pyrochlore structure. *Chemistry letters*. 2004;33(8):954-5.
144. Higashi M, Abe R, Sayama K, Sugihara H, Abe Y. Improvement of photocatalytic activity of titanate pyrochlore Y₂Ti₂O₇ by addition of excess Y. *Chemistry letters*. 2005;34(8):1122-3.
145. Reddy VR, Hwang DW, Lee JS. Effect of Zr substitution for Ti in KLaTiO₄ for photocatalytic water splitting. *Catalysis letters*. 2003;90(1-2):39-43.
146. Kudo A, Okutomi H, Kato H. Photocatalytic water splitting into H₂ and O₂ over K₂LnTa₅O₁₅ powder. *Chemistry letters*. 2000;29(10):1212-3.
147. Takata T, Furumi Y, Shinohara K, Tanaka A, Hara M, Kondo JN, *et al.* Photocatalytic decomposition of water on spontaneously hydrated layered perovskites. *Chemistry of materials*. 1997;9(5):1063-4.
148. Sreethawong T, Suzuki Y, Yoshikawa S, editors. Improved photocatalytic hydrogen evolution over mesoporous Ni/TiO₂ prepared by single-step sol-gel technique with surfactant template. *Electron Transfer in Nanomaterials: Proceedings of the International Symposium*;

- 2006: The Electrochemical Society.
149. Kato H, Kudo A. New tantalate photocatalysts for water decomposition into H₂ and O₂. *Chemical Physics Letters*. 1998;295(5-6):487-92.
150. Hong SJ, Jun H, Lee JS. Nanocrystalline WO₃ film with high photo-electrochemical activity prepared by polymer-assisted direct deposition. *Scripta Materialia*. 2010;63(7):757-60.
151. Chatchai P, Murakami Y, Kishioka S-y, Nosaka AY, Nosaka Y. Efficient photocatalytic activity of water oxidation over WO₃/BiVO₄ composite under visible light irradiation. *Electrochimica Acta*. 2009;54(3):1147-52.
152. Chatchai P, Kishioka S-y, Murakami Y, Nosaka AY, Nosaka Y. Enhanced photoelectrocatalytic activity of FTO/WO₃/BiVO₄ electrode modified with gold nanoparticles for water oxidation under visible light irradiation. *Electrochimica acta*. 2010;55(3):592-6.
153. Chatchai P, Murakami Y, Kishioka S-y, Nosaka A, Nosaka Y. FTO/SnO₂/BiVO₄ composite photoelectrode for water oxidation under visible light irradiation. *Electrochemical and Solid-State Letters*. 2008;11(6):H160-H3.
154. Byun S, Kim B, Jeon S, Shin B. Effects of a SnO₂ hole blocking layer in a BiVO₄-based photoanode on photoelectrocatalytic water oxidation. *Journal of Materials Chemistry A*. 2017;5(15):6905-13.
155. Xia L, Bai J, Li J, Zeng Q, Li L, Zhou B. High-performance BiVO₄ photoanodes cocatalyzed with an ultrathin α-Fe₂O₃ layer for photoelectrochemical application. *Applied Catalysis B: Environmental*. 2017;204:127-33.
156. Kim JH, Jang J-W, Jo YH, Abdi FF, Lee YH, Van De Krol R, *et al.* Hetero-type dual photoanodes for unbiased solar water splitting with extended light harvesting. *Nature communications*. 2016;7(1):1-9.
157. Pilli SK, Deutsch TG, Furtak TE, Brown LD, Turner JA, Herring AM. BiVO₄/CuWO₄ heterojunction photoanodes for efficient solar driven water oxidation. *Physical chemistry chemical physics*. 2013;15(9):3273-8.
158. Li L-P, Liu M, Zhang W-D. Electrodeposition of CdS onto BiVO₄ films with high photoelectrochemical performance. *Journal of Solid State Electrochemistry*. 2018;22(8):2569-77.
159. Jiang J, Wang M, Li R, Ma L, Guo L. Fabricating CdS/BiVO₄ and BiVO₄/CdS heterostructured film photoelectrodes for photoelectrochemical applications. *International journal of hydrogen energy*. 2013;38(29):13069-76.
160. Su J, Guo L, Bao N, Grimes CA. Nanostructured WO₃/BiVO₄ heterojunction films for efficient photoelectrochemical water splitting. *Nano letters*. 2011;11(5):1928-33.
161. Moniz SJ, Zhu J, Tang J. 1D Co-Pi modified BiVO₄/ZnO junction cascade for efficient photoelectrochemical water cleavage. *Advanced Energy Materials*. 2014;4(10):1301590.
162. Ho-Kimura S, Moniz SJ, Handoko AD, Tang J. Enhanced photoelectrochemical water splitting by nanostructured BiVO₄-TiO₂ composite electrodes. *Journal of Materials Chemistry A*. 2014;2(11):3948-53.
163. Gurunathan K, Maruthamuthu P, Sastri M. Photocatalytic hydrogen production by dye-sensitized Pt/SnO₂ and Pt/SnO₂/RuO₂ in aqueous methyl viologen solution. *International Journal of Hydrogen Energy*. 1997;22(1):57-62.
164. Dhanalakshmi K, Latha S, Anandan S, Maruthamuthu P. Dye sensitized hydrogen evolution from water. *International Journal of Hydrogen Energy*. 2001;26(7):669-74.
165. Polo AS, Itokazu MK, Iha NYM. Metal complex sensitizers in dye-sensitized solar cells. *Coordination Chemistry Reviews*. 2004;248(13-14):1343-61.
166. Bi Z-C, Tien HT. Photoproduction of hydrogen by dye-sensitized systems. *International Journal of Hydrogen Energy*. 1984;9(8):717-22.
167. Ni M, Leung MK, Leung DY, Sumathy K. A review and recent developments in photocatalytic water-splitting using TiO₂ for hydrogen production. *Renewable and Sustainable Energy Reviews*. 2007;11(3):401-25.
168. Gole JL, Stout JD, Burda C, Lou Y, Chen X. Highly efficient formation of visible light tunable TiO₂-x N x photocatalysts and their transformation at the nanoscale. *The journal of physical chemistry B*. 2004;108(4):1230-40.
169. Mrowetz M, Balcerski W, Colussi A, Hoffmann

- MR. Oxidative power of nitrogen-doped TiO₂ photocatalysts under visible illumination. *The Journal of Physical Chemistry B*. 2004;108(45):17269-73.
170. Wu N-L, Lee M-S. Enhanced TiO₂ photocatalysis by Cu in hydrogen production from aqueous methanol solution. *International Journal of Hydrogen Energy*. 2004;29(15):1601-5.
171. Szabó-Bárdos E, Czili H, Horváth A. Photocatalytic oxidation of oxalic acid enhanced by silver deposition on a TiO₂ surface. *Journal of Photochemistry and Photobiology A: Chemistry*. 2003;154(2-3):195-201.
172. Anpo M, Takeuchi M. The design and development of highly reactive titanium oxide photocatalysts operating under visible light irradiation. *Journal of catalysis*. 2003;216(1-2):505-16.
173. Subramanian V, Wolf EE, Kamat PV. Catalysis with TiO₂/gold nanocomposites. Effect of metal particle size on the Fermi level equilibration. *Journal of the American Chemical Society*. 2004;126(15):4943-50.
174. Subramanian V, Wolf EE, Kamat PV. Green emission to probe photoinduced charging events in ZnO– Au nanoparticles. Charge distribution and Fermi-level equilibration. *The Journal of Physical Chemistry B*. 2003;107(30):7479-85.
175. Jakob M, Levanon H, Kamat PV. Charge distribution between UV-irradiated TiO₂ and gold nanoparticles: determination of shift in the Fermi level. *Nano letters*. 2003;3(3):353-8.
176. Bamwenda GR, Tsubota S, Nakamura T, Haruta M. Photoassisted hydrogen production from a water-ethanol solution: a comparison of activities of Au· TiO₂ and Pt· TiO₂. *Journal of Photochemistry and Photobiology A: Chemistry*. 1995;89(2):177-89.
177. Sakthivel S, Shankar M, Palanichamy M, Arabindoo B, Bahnemann D, Murugesan V. Enhancement of photocatalytic activity by metal deposition: characterisation and photonic efficiency of Pt, Au and Pd deposited on TiO₂ catalyst. *Water research*. 2004;38(13):3001-8.
178. Balandin AA, Ghosh S, Bao W, Calizo I, Teweldebrhan D, Miao F, *et al.* Superior thermal conductivity of single-layer graphene. *Nano letters*. 2008;8(3):902-7.
179. Martin J, Akerman N, Ulbricht G, Lohmann T, Smet Jv, Von Klitzing K, *et al.* Observation of electron–hole puddles in graphene using a scanning single-electron transistor. *Nature physics*. 2008;4(2):144-8.
180. Zhang X-Y, Li H-P, Cui X-L, Lin Y. Graphene/TiO₂ nanocomposites: synthesis, characterization and application in hydrogen evolution from water photocatalytic splitting. *Journal of Materials Chemistry*. 2010;20(14):2801-6.
181. Xie H, Hou C, Wang H, Zhang Q, Li Y. S, N co-doped graphene quantum dot/TiO₂ composites for efficient photocatalytic hydrogen generation. *Nanoscale research letters*. 2017;12(1):400.
182. Fan W, Lai Q, Zhang Q, Wang Y. Nanocomposites of TiO₂ and reduced graphene oxide as efficient photocatalysts for hydrogen evolution. *The Journal of Physical Chemistry C*. 2011;115(21):10694-701.
183. Hao X, Jin Z, Xu J, Min S, Lu G. Functionalization of TiO₂ with graphene quantum dots for efficient photocatalytic hydrogen evolution. *Superlattices and Microstructures*. 2016;94:237-44.
184. Zhang K, Jing D, Xing C, Guo L. Significantly improved photocatalytic hydrogen production activity over Cd_{1-x}Zn_xS photocatalysts prepared by a novel thermal sulfuration method. *International Journal of Hydrogen Energy*. 2007;32(18):4685-91.
185. Zahraa MBaO. Photocatalytic reactors. *International Journal Of Photoenergy*. 2003;05.
186. Hisatomi T, Domen K. Reaction systems for solar hydrogen production via water splitting with particulate semiconductor photocatalysts. *Nature Catalysis*. 2019;2(5):387-99.
187. Nguyen T-V, Wu JC. Photoreduction of CO₂ to fuels under sunlight using optical-fiber reactor. *Solar energy materials and solar cells*. 2008;92(8):864-72.
188. Ola O, Maroto-Valer MM. Review of material design and reactor engineering on TiO₂ photocatalysis for CO₂ reduction. *Journal of Photochemistry and Photobiology C: Photochemistry Reviews*. 2015;24:16-42.
189. Hu Y, Xu J, Yuan C, Lin J, Yin Z. A single

- TiO₂-coated side-glowing optical fiber for photocatalytic wastewater treatment. *Chinese Science Bulletin*. 2005;50(18):1979-84.
190. Tahir M, Tahir B, Amin NS. Photocatalytic CO₂ reduction by CH₄ over montmorillonite modified TiO₂ nanocomposites in a continuous monolith photoreactor. *Materials Research Bulletin*. 2015;63:13-23.
191. Boyjoo Y, Sun H, Liu J, Pareek VK, Wang S. A review on photocatalysis for air treatment: from catalyst development to reactor design. *Chemical Engineering Journal*. 2017;310:537-59.
192. Gaudillere C, González JJ, Chica A, Serra JM. YSZ monoliths promoted with Co as catalysts for the production of H₂ by steam reforming of ethanol. *Applied Catalysis A: General*. 2017;538:165-73.
193. Tahir M, Amin NS. Photocatalytic CO₂ reduction and kinetic study over In/TiO₂ nanoparticles supported microchannel monolith photoreactor. *Applied Catalysis A: General*. 2013;467:483-96.
194. Tahir M, Amin NS. Performance analysis of nanostructured NiO-In₂O₃/TiO₂ catalyst for CO₂ photoreduction with H₂ in a monolith photoreactor. *Chemical Engineering Journal*. 2016;285:635-49.
195. Pinaud BA, Benck JD, Seitz LC, Forman AJ, Chen Z, Deutsch TG, *et al.* Technical and economic feasibility of centralized facilities for solar hydrogen production via photocatalysis and photoelectrochemistry. *Energy & Environmental Science*. 2013;6(7):1983-2002.
196. Setoyama T, Takewaki T, Domen K, Tatsumi T. The challenges of solar hydrogen in chemical industry: how to provide, and how to apply? *Faraday discussions*. 2017;198:509-27.
197. Jing D, Liu H, Zhang X, Zhao L, Guo L. Photocatalytic hydrogen production under direct solar light in a CPC based solar reactor: reactor design and preliminary results. *Energy Conversion and Management*. 2009;50(12):2919-26.
198. Tahir M, Amin NS. Recycling of carbon dioxide to renewable fuels by photocatalysis: Prospects and challenges. *Renewable and Sustainable Energy Reviews*. 2013;25:560-79.
199. Lin H, Valsaraj KT. An optical fiber monolith reactor for photocatalytic wastewater treatment. *AIChE Journal*. 2006;52(6):2271-80.
200. Al-Hamdi AM, Rinner U, Sillanpää M. Tin dioxide as a photocatalyst for water treatment: a review. *Process Safety and Environmental Protection*. 2017;107:190-205.
201. Puga AV. Photocatalytic production of hydrogen from biomass-derived feedstocks. *Coordination Chemistry Reviews*. 2016;315:1-66.
202. Ahmad H, Kamarudin S, Minggu L, Kassim M. Hydrogen from photo-catalytic water splitting process: A review. *Renewable and Sustainable Energy Reviews*. 2015;43:599-610.
203. Baniasadi E, Dincer I, Naterer G. Performance analysis of a water splitting reactor with hybrid photochemical conversion of solar energy. *International journal of hydrogen energy*. 2012;37(9):7464-72.
204. Tambago HMG, de Leon RL. Intrinsic kinetic modeling of hydrogen production by photocatalytic water splitting using cadmium zinc sulfide catalyst. *Int J Chem Eng Appl*. 2015;6:220-7.
205. Kumar DP, Kumari VD, Karthik M, Sathish M, Shankar M. Shape dependence structural, optical and photocatalytic properties of TiO₂ nanocrystals for enhanced hydrogen production via glycerol reforming. *Solar Energy Materials and Solar Cells*. 2017;163:113-9.
206. Boudjemaa A, Rebahi A, Terfassa B, Chebout R, Mokrani T, Bachari K, *et al.* Fe₂O₃/carbon spheres for efficient photo-catalytic hydrogen production from water and under visible light irradiation. *Solar Energy Materials and Solar Cells*. 2015;140:405-11.
207. Huaxu L, Fuqiang W, Ziming C, Shengpeng H, Bing X, Xiangtao G, *et al.* Analyzing the effects of reaction temperature on photo-thermo chemical synergetic catalytic water splitting under full-spectrum solar irradiation: an experimental and thermodynamic investigation. *International Journal of Hydrogen Energy*. 2017;42(17):12133-42.
208. Zhang Z, Maggard PA. Investigation of photocatalytically-active hydrated forms of amorphous titania, TiO₂•nH₂O. *Journal of Photochemistry and Photobiology A: Chemistry*. 2007;186(1):8-13.

209. Liu S, Luo Z, Li L, Li H, Chen M, Wang T, *et al.* Multifunctional TiO₂ overlayer for p-Si/n-CdS heterojunction photocathode with improved efficiency and stability. *Nano Energy*. 2018;53:125-9.
210. Brahimi R, Bessekhoud Y, Bouguelia A, Trari M. CuAlO₂/TiO₂ heterojunction applied to visible light H₂ production. *Journal of Photochemistry and Photobiology A: Chemistry*. 2007;186(2-3):242-7.
211. Maeda K. Photocatalytic properties of rutile TiO₂ powder for overall water splitting. *Catalysis Science & Technology*. 2014;4(7):1949-53.
212. Fujita S-i, Kawamori H, Honda D, Yoshida H, Arai M. Photocatalytic hydrogen production from aqueous glycerol solution using NiO/TiO₂ catalysts: Effects of preparation and reaction conditions. *Applied Catalysis B: Environmental*. 2016;181:818-24.
213. Nada A, Hamed H, Barakat M, Mohamed N, Veziroglu T. Enhancement of photocatalytic hydrogen production rate using photosensitized TiO₂/RuO₂-MV²⁺. *International journal of hydrogen energy*. 2008;33(13):3264-9.
214. Lu J, Wang Y, Huang J, Fei J, Cao L, Li C. In situ synthesis of mesoporous C-doped TiO₂ single crystal with oxygen vacancy and its enhanced sunlight photocatalytic properties. *Dyes and Pigments*. 2017;144:203-11.
215. Zhang D, Ma X, Zhang H, Liao Y, Xiang Q. Enhanced photocatalytic hydrogen evolution activity of carbon and nitrogen self-doped TiO₂ hollow sphere with the creation of oxygen vacancy and Ti³⁺. *Materials today energy*. 2018;10:132-40.
216. Méndez JO, López CR, Melián EP, Díaz OG, Rodríguez JD, Hevia DF, *et al.* Production of hydrogen by water photo-splitting over commercial and synthesised Au/TiO₂ catalysts. *Applied Catalysis B: Environmental*. 2014;147:439-52.
217. Chen W-T, Chan A, Al-Azri ZH, Dosado AG, Nadeem MA, Sun-Waterhouse D, *et al.* Effect of TiO₂ polymorph and alcohol sacrificial agent on the activity of Au/TiO₂ photocatalysts for H₂ production in alcohol–water mixtures. *Journal of catalysis*. 2015;329:499-513.
218. Police AKR, Basavaraju S, Valluri DK, Machiraju S, Lee JS. CaFe₂O₄ sensitized hierarchical TiO₂ photo composite for hydrogen production under solar light irradiation. *Chemical engineering journal*. 2014;247:152-60.
219. Umer M, Tahir M, Azam MU, Jaffar MM. Metals free MWCNTs@ TiO₂@ MMT heterojunction composite with MMT as a mediator for fast charges separation towards visible light driven photocatalytic hydrogen evolution. *Applied Surface Science*. 2019;463:747-57.
220. López-Tenllado F, Hidalgo-Carrillo J, Montes V, Marinas A, Urbano F, Marinas J, *et al.* A comparative study of hydrogen photocatalytic production from glycerol and propan-2-ol on M/TiO₂ systems (M= Au, Pt, Pd). *Catalysis Today*. 2017;280:58-64.
221. Cao B, Li G, Li H. Hollow spherical RuO₂@ TiO₂@ Pt bifunctional photocatalyst for coupled H₂ production and pollutant degradation. *Applied Catalysis B: Environmental*. 2016;194:42-9.
222. Al-Azri ZH, Chen W-T, Chan A, Jovic V, Ina T, Idriss H, *et al.* The roles of metal co-catalysts and reaction media in photocatalytic hydrogen production: Performance evaluation of M/TiO₂ photocatalysts (M= Pd, Pt, Au) in different alcohol–water mixtures. *Journal of catalysis*. 2015;329:355-67.
223. Li Y, Wang B, Liu S, Duan X, Hu Z. Synthesis and characterization of Cu₂O/TiO₂ photocatalysts for H₂ evolution from aqueous solution with different scavengers. *Applied Surface Science*. 2015;324:736-44.